Universidade de Aveiro Departamento de Química
2011

Patrícia Isabel Duarte de Figueiredo

Leaf lettuce metabolome during aging and under stress

Universidade de Aveiro Departamento de Química
2011

Patrícia Isabel Duarte de Figueiredo

Leaf lettuce metabolome during aging and under stress

Dissertation submitted to the University of Aveiro to fulfil the requirements for the degree of Master in the field of Biotechnology, done under the scientific supervision of Doctor Ana Maria Pissarra Coelho Gil, Associated Professor with Aggregation of the Department of Chemistry and of Doctor Maria Celeste Pereira Dias, Post-Doctoral fellow of the Department of Biology of the University of Aveiro.

Examining Committee

president

Prof. Doctor João Manuel da Costa e Araújo Pereira Coutinho
Associated Professor with Aggregation of the Department of Chemistry of the University of Aveiro

Prof. Doctor Ana Maria Pissara Coelho Gil
Associated Professor with Aggregation of the CICECO/Department of Chemistry of the University of Aveiro

Doctor Maria Celeste Pereira Dias
Post-Doctoral fellow of the Department of Biology of the University of Aveiro

Prof. Doctor Maria da Conceição Lopes Vieira dos Santos
Associated Professor with Aggregation of the Department of Biology of the University of Aveiro

Doctor Iola Melissa Fernandes Duarte
Auxiliary Researcher of the CICECO of the University of Aveiro

Acknowledgements

This work would not have been completed without help and support of many.
I owe my deepest gratitude to my supervisor Doctor Ana Gil and Doctor Celeste Dias for their guidance and support.
I would like to express my gratitude to Doctor Iola Duarte for all assistance given.
I wish to acknowledge the center of the Rede Nacional de Ressonância Magnética (CERMAX).
I am grateful to everyone in the Metabonomics group of the university of Aveiro, and to Inês Lamego for all the help and availability.
To my good friends, Cristina Barros and Filipa Silva, whose supports made this thesis possible.
Lastly, my family without whose support none of this would have been possible and to Rui for all the patience and kindness, because you are my only exception.

palavras-chave

Alface, Envelhecimento, Luz, Metabonómica, Pesticidas, Ressonância Magnética Nuclear.

resumo

O metaboloma das plantas é extremamente diverso devido à enorme variedade de metabolitos secundários. A espectroscopia de ressonância magnética nuclear (RMN) é cada vez mais utilizada na metabonómica, na identificação dos metabolitos presentes nas plantas quando estas se encontram sob stress. O trabalho apresentado nesta tese teve como objetivo avaliar as alterações metabólicas e fisiológicas que ocorreram na folha da alface causadas pelo envelhecimento, por condições de crescimento na luz e no escuro e devido à exposição ao pesticida mancozebe. As alfaces cresceram durante quatro semanas, e foram depois separadas em dois grupos de forma a estudar as condições luz/escuro e exposição ao pesticida mancozebe durante o crescimento. No estudo das condições luz/escuro algumas alfaces foram expostas durante uma semana a luz de intensidade de 200 ± 20 $\mu mol.m^{-2}.s^{-1}$ (controlo) e outras a 20 ± 20 $\mu mol.m^{-2}.s^{-1}$ (condições no escuro). Nos ensaios com o pesticida, foi aplicado o mancozebe a um conjunto de alfaces e ao outro não (controlo). Após uma semana, recolheu-se as folhas novas (primeiro nó) e folhas expandidas (nó apical).

Em geral, os resultados mostram que a idade da folha, as condições de luz e a exposição ao mancozebe influenciam, tanto o desempenho fisiológico da planta, ou seja, concentração de pigmentos e eficiência fotossintética, como a composição metabólica da planta. Os resultados mostram que as folhas jovens têm maiores teores de glucose e sacarose, e menor teor de ácido málico e cítrico que as folhas expandidas, e que não houve diferenças significativas nos parâmetros fisiológicos medidos. No escuro, as folhas de alface apresentam uma diminuição na performance fotossintética, que foi mais acentuada nas folhas expandidas em comparação com folhas jovens, resultando em reduções significativas de glucose e sacarose nessas folhas. Além disso, a exposição de folhas de alface ao mancozebe resultou na diminuição da performance fotossintética, mais acentuada em folhas expandidas do que nas folhas jovens, com acumulação de glucose e decréscimo de alguns aminoácidos e vários ácidos orgânicos.

keywords

Lettuce, Aging, Light, Metabonomics, Pesticides, Nuclear Magnetic Resonance.

abstract

The plant metabolome is extremely diverse due to the extraordinary variety of secondary metabolites. Nuclear magnetic resonance (NMR) spectroscopy techniques in metabonomics have been used for the identification of metabolite presents in plants under stress. The work reported in this thesis aimed to evaluate the metabolic and physiological changes that occur in lettuce leaves, caused by aging, light and dark growth conditions and due to exposure to mancozeb pesticide. Lettuces were grown during four weeks, and then separated in two groups in order to study the light/dark conditions and mancozeb pesticide exposure during growth. For the light/dark conditions study some lettuces were exposed during one week to a light intensity of 200 ± 20 $\mu mol.m^{-2}.s^{-1}$ (control), and others to 20 ± 20 $\mu mol.m^{-2}.s^{-1}$ (dark conditions). In the pesticide assay, the mancozeb was applied to a set of lettuces and not to the other (control). After one week, young leaves (from the first node) and expanded leaves (from the apical node) were collected.

In general, the results show that the leaf age, the light/dark conditions and the exposure to mancozeb influence the plant physiological performance, such as pigment concentration and photosynthetic efficiency, as well as the plant metabolomic composition. The results show that young leaves show higher contents of glucose and sucrose, and lower contents of malic and citric acids than expanded leaves, and there was no significant differences in the physiological parameters measured. In the dark, the lettuce leaves present a decreased in the photosynthetic performance, which was more marked in expanded leaves compared to young leaves, resulting in significant decreases of glucose and sucrose on these leaves. Moreover, exposure of lettuce leaves with mancozeb resulted in decrease in photosynthetic performance, more marked in expanded leaves than in young leaves, with accumulation of glucose and decrease in some amino acids and several organic acids.

Contents

Abbreviations

1D	One-dimensional
2D	Two-dimensional
Chl *a*	Chlorophyll *a*
Chl *b*	Chlorophyll *b*
COSY	Correlation Spectroscopy
DTCs	Dithiocarbamates
EBDCs	Ethylenebis(dithiocarbamates)
EDA	Ethylenediamine
EDTA	Disodium ethylenediaminetetraacetic acid
ETU	Ethylenethiourea
EU	Euthyleneurea
F_0	Minimal Fluorescence
F_m	Maximal Fluorescence
GC	Gas Chromatography
HRMAS	High Resolution Magic Angle Spinning
HSQC	Heteronuclear single-quantum correlation
LC	Liquid Chromatography
MAS	Magic Angle Spinning
MS	Mass Spectrometry
NMR	Nuclear Magnetic Resonance
OSC	Orthogonal Signal Correction
PC	Principal Component
PCA	Principal Component Analysis
PLS	Partial Least Squares
PLS-DA	Partial Least Squares - Discriminant Analysis
PSII	Photosystem II
TOCSY	Total Correlation Spectroscopy

1. Introduction

1.1. General Considerations about Lettuce

1.1.1. Biological classification and chemical composition

Lettuce is an annual herbaceous plant which belongs to the family of the Asteraceae, genus *Lactuca* and species *Lactuca sativa.* This species has a relatively small root system close to the surface, thus is dependent upon fertile, water-retentive soil and a pH of between 6.0 and 7.0 is satisfactory for a best growth. In general the cultivar groups of lettuce are differentiated by head formation and leaf structure, and the most commonly recognized are the Butterhead *(L. sativa* var. *capitata)*, the Chinese *(L. sativa* var. *asparagina),* the Crisphead, the Looseleaf *(L. sativa* var. *crispa)*, the Romaine *(L. sativa* var. *romana),* and the Summer Crisp (Ferreira, 2007; Kumar *et al.*, 2010).

This species was first used in the Mediterranean region, in the South of Europe, and in the Occidental Asia for medicine purposes (Romani *et al.*, 2002). Nowadays, lettuce is a high-value leafy vegetable that is grown worldwide, widespread globally and is one of the most consumed leafy vegetables in human diet because of its high nutritional value. As a matter of fact, some studies have revealed the importance of lettuce in preventing cardiovascular diseases in rats and humans (Nicolle *et al.*, 2004; Serafini *et al.*, 2002).

Considering its chemical composition, on average, 350 g of lettuce has 56 kilocalories, and 96% of water, 2.3% carbohydrates, 1.2% of protein, 0.2% fat and vitamin A, vitamin B, vitamin C, vitamin K and iron (Ferreira, 2007; Tavares, 1988). The major carbohydrates present in lettuce are glucose, fructose and sucrose (Sobolev *et al.*, 2005). The phenolic compounds in lettuce have an important role in the antioxidant activity, since the dominant antioxidants in lettuce, being caffeic acid derivatives and flavonoids, arises from a number of phenolic compounds. The main phenolic compounds present in lettuce are monocaffeoyltartaric acid, chicoric acid, chlorogenic acid and 3,5-di-0-caffeoylquinic acid (Romani *et al.*, 2002). Together with the antioxidant molecules content, the phenolic compounds (0.5-2 mg/fresh weight) in this species depend on the cultivar and on the ripening stage (DuPont *et al.*, 2000; Fukumoto *et al.*, 2002; Oh *et al.*, 2009). Malic, citric, fumaric, formic, acetic, succinic, lactic, α-ketoglutaric and ascorbic acid are some of the organic acids found in the lettuce. Some of the amino acids found are alanine, glutamate, glutamine, threonine and valine. The content and composition of chlorophylls and their

derivative depend on the leaf position at the shoot. Lutein and β-carotene are the main carotenoids present in lettuce. The minor carotenoids found in lettuce are the neoxanthin, violaxanthin and lactucaxanthin (Kimura and Rodriguez-Amaya, 2003). Fatty acids are present in lettuce in trace levels, mainly as palmitic, stearic acid, oleic, linoleic or linolenic acid (Romani *et al.*, 2002; Winter and Herrmann, 1986).

1.1.2. Biomarkers and lettuce as a model in plant toxicology

For long, the first toxicology tests were focused on the effect of chemicals on human health and safety (Krieger, 2010). In the last decades, interest has expanded to other areas such as the study of putative accumulation through trophic chains, and in water/soil and consequent environmental impact. This impact is evaluated through the use of dose/response bioassays (Krieger, 2010). For bioassays designed to estimate toxicity to humans, organisms, such as laboratory rats and mice are commonly used because their response to chemical exposures provides a reasonable model of human response.

Concerning the environmental bioassays, the species of choice may depend on the type of chemicals being studied and the purpose of the experiments (Trautmann *et al.*, 2001). Lettuce is used in environmental bioassays, since this species, is known to be greatly sensitive to common environmental contaminants such as heavy metals, pesticides, solvents, and other types of environmental stresses. In addition, this species is consumed throughout the world. Thus, it is important assess the effect of contamination of this crop because its consumption may represent a risk to human health. Furthermore, in general higher plants offer several benefits for *in situ* monitoring and screening of environmental toxicity. For all these reasons, the lettuce is a species recommended for standard toxicity tests. Besides this, it is a crop that it is easy to handle, and results are easily transposed to the dicotyledonous species (Gaw *et al.*, 2008; Huang, *et al.*, 2004; ISO, 1993 and 1995; Monteiro *et al.*, 2010).

The selection of putatively ideal biomarkers in plant toxicology remains one of the most important issues today. Besides, the traditionally recommended oxidative stress, obviously related to stress imbalances, it has been proposed the inclusion of photosynthetic related parameters (Razinger *et al.*, 2009).

Photosynthesis is a complex process in which plants converts carbon dioxide into organic compounds, mainly sugars, involving light-dependent and carbon-assimilation reactions in the chloroplasts (Rosa *et al.,* 2009). In particular, the light-dependent reactions take place in the thylakoids, an internal compartment in the chloroplasts, in which are embedded the photosynthetic pigments and the enzyme complexes that carry out these reactions. Plants exposed to stress resulting in an inhibition, for example, in the photosynthetic pigments synthesis may present considerable differences in the relative composition of these pigments, such as chlorophyll *a* (chl *a*), chlorophyll *b* (chl *b*) and carotenoids (Lichtenthaler *et al.,* 2007). For photophosphorylation, pigments content and their photosynthetic efficiency, in particular the photosystems functionality is crucial. In particular, the status of oxidation/reduction of the photosystem II (PSII) is recommended as a biomarker (Monteiro *et al.*, 2009).

There are few studies that describe the uptake of contaminants, such as metals and pesticides, and the effects triggered by them in lettuce (e.g. Dias *et al.*, 2011; Monteiro *et al.*, 2009; Untiedt and Blanke, 2004; Zorrig *et al.,* 2010). These studies point that the photosynthetic apparatus of lettuce is very sensitive to those stresses and the photosynthetic parameters used revealed to be sensible biomarkers to assess the toxicity of these compounds. Moreover, these studies in lettuce promoted the identification of several photosynthetic targets of these toxic compounds. Monteiro *et al.* (2009), for example, studied the uptake and toxicity effects of cadmium (Cd), in young and expanded lettuce leaves through the measurement of different parameters, such as chlorophyll *a* fluorescence, pigment content and shoot and root growth. The results showed that lettuce leaves and roots are very sensitive to Cd toxicity since they can accumulate high levels of Cd. Moreover, Cd exposure promotes a decrease on the photosynthetic efficiency (F_v/F_m) of expanded leaves due to the significant decrease on chlorophyll content compared to control leaves. In addition, the expanded leaves exposed to Cd presented a significant decrease on other chlorophyll *a* fluorescence parameters (e.g. F_0 and F_m) when compared to control leaves. Young leaves seem to be less sensitive to Cd toxicity. Furthermore, Cd induced a decrease in shoot growth and root growth after 14 days of exposure.

1.2. Dithiocarbamate Pesticides

The present work was focused on the study on the effect of mancozeb application in lettuce. The mancozeb is a dithiocarbamate pesticide (DTCs). The DTCs were chosen because the annual report of pesticides residues performed by the European Union demonstrates that the residues from DTCs are one of the most commonly found in the lettuce (EFSA, 2009). In addition, the mancozeb was chosen because this fungicide is widely used in Portugal and may be used in this species to prevent mildew disease (Mukerji, 2004).

DTCs are mainly used in agriculture and form part of the large group of carbamates that have been developed and produced on a large scale in the last 40 to 50 years (Krieger, 2010). Furthermore, the DTCs are used as fungicides, because of the effectiveness against a broad spectrum of fungi and plant diseases caused by them (Houeto *et al.*, 1995) and because they have high water solubility which allows them to be taken up by the roots and into the leaves of plants (EHU, 2002). The mancozeb (illustrated in Figure 1.1) belongs to the ethylenebisdithiocarbamates (EBDCs) group (Crnogorac and Schwack, 2009).

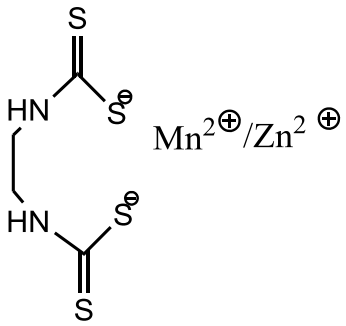

Figure 1.1: Illustration of the structure of mancozeb. Adapted from Caldas *et al.* (2004).

The modes by which EBDCs elicit toxicity, besides the inhibition of cholinesterase enzymes, include the capacity to deactivate the sulfhydril containing enzymes, the ATP production and the Krebs cycle. The metabolism of mancozeb in laboratory animals show that the EBDCs are partially absorbed, rapidly metabolized and excreted without long-term bioaccumulation. Only low level residues are found in the thyroid (Merhi *et al.*, 2010). The major metabolite detected was the ethylenethiourea (ETU), responsible for making EBDCs carcinogenic (Krieger, 2010).

In Figure 1.2 is illustrated the metabolites produced in laboratory animals, resulting from two common metabolic pathways. In the first metabolic pathway the EBDC linkages is hydrolyzed producing ethylenediamine (EDA), which is oxidized to glycine. The other pathway is responsible for the toxic effects of the EBDCs and involves oxidation to EBIS and after that to ETU and Ethyleneurea (EU) before return to the main pathway with conversion to EDA, glycine, pyruvate and other natural products. The conversion of mancozeb to EBDCs and after to EDA are recognized chemical, non-enzymatic reactions (Blasco *et al.*, 2004; Mulkey, 2001).

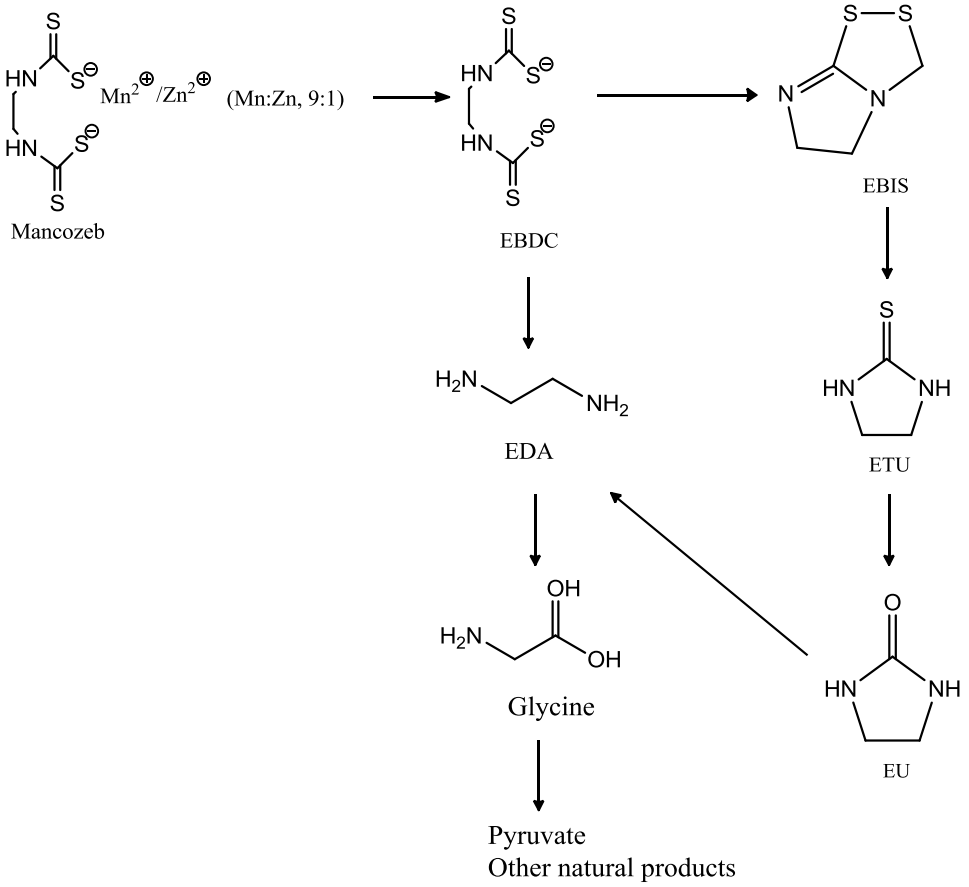

Figure 1.2: Metabolic pathway of mancozeb. Adapted from Mulkey (2001).

Although the focus of the present study was not to determine DTCs and their residues, some of the methods for their determination are discussed briefly. The predominant method for determining DTCs and their residues is based on the methods of digestion/distillation of DTCs to carbon disulphide (CS_2) in an acid medium, combined with spectrophotometry. However, these methods are usually slow, insensitive, and imprecise since while distinguish between the subclasses of DTCs, for example, sometimes

the crops of phytogenic CS_2 (e.g. broccoli and cabbage) sources give false-positives CS_2 contents. Nevertheless, these methods are still used as a way to measure the presence of DTCs in crops followed by gas chromatography (GC) and electron-capture or flame-photometric detection to confirm spectrophotometric results (Blasco *et al.,* 2004; Crnogorac and Schwack, 2009).

Although the methods described above remain the predominant methods for determination of DTCs, there are other methods for direct determination of DTCs anion, that give rise to more rapid and sensitive analysis while avoiding false-positive results. For example, van Lishaut and Schwack (2000) used liquid chromatography (LC) with ultraviolet and electrochemical detection to determine all three DTCs subclasses.

An additional method used for determination of DTCs is LC coupled with mass spectrometry (MS) method, for example, Crnogorac and Schwack (2007) study all threes subclasses of DTCs through the use of this method, Brewin *et al.* (2008) published an LC coupled with mass spectrometry tandem method for the determinations of EBDCs and Lin *et al.* (2011) described a dispersive liquid–liquid micro-extraction coupled with high performance liquid chromatography-diode array detection method for the determination of *N*-methylcarbamates, in some vegetables, including the lettuce.

1.3. Plant Metabonomics Approaches

1.3.1. Global methodology

The term metabonomics, originated in the late 90´s, can be defined as "*the quantitative measurement of the dynamic multiparametric metabolic response of living systems to pathophysiological stimuli or genetic modification"* (Nicholson *et al.,* 1999; Oliver *et al.,* 1998).

This approach aims to detect, identify, and quantify the metabolic changes that occur in the samples analysed as a result of toxic insult, disease, genetic handling or environmental stress, and as a response to clinical intervention with drugs or other therapy (Alam *et al.,* 2010; Graça *et al.,* 2009; Griffin, 2004; Krishnan *et al.,* 2005; Nielsen and Jewett, 2007).

Metabonomics measures the metabolome, which covers the complete set of

metabolites (Colquhoun, 2007; Nielsen and Jewett, 2007), and is widely applied in the study of biofluids (Graça *et al.,* 2009), cells (Beger *et al.,* 2010), and tissue extracts (Duarte *et al.,* 2010). In addition, the metabonomics studies have also been applied to plants because they have a variety of secondary metabolites which makes their metabolome extremely diverse (Colquhoun, 2007; Ward *et al.,* 2007).

The metabonomics approach involves analytical technologies and chemometric methods. Concerning the analytical technologies used in metabonomics the most widely used techniques are the GC-MS and Nuclear Magnetic Resonance (NMR) spectroscopy because the spectra delivers high-density information on a wide range of biochemical pathways, simultaneously with high analytical precision (Griffiths and Wang, 2008; Lindon and Nicholson, 2008; Sumner *et al.,* 2003; Villas-Bôas *et al.,* 2005). Figure 1.3 presents a schematic workflow of a metabonomics approach from tissue harvest through to data interpretation using MS or NMR.

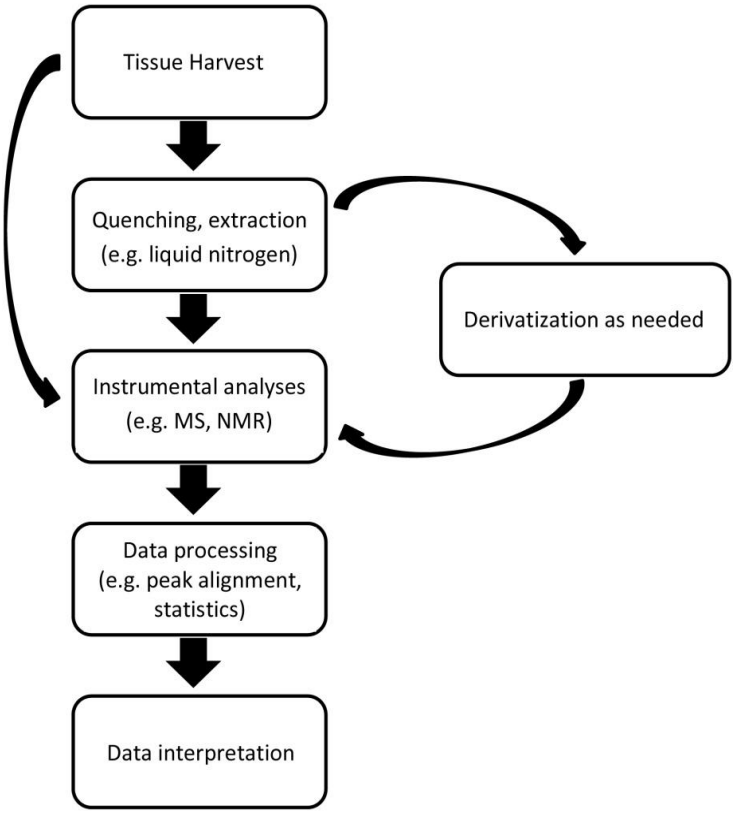

Figure 1.3: Schematic workflow of a metabonomics approach from tissue harvest through to data interpretation. Adapted from Schwender (2009).

When working with plant metabolites, ideally all sampling should be conducted at the same time of the day. Then, it is important to quench the metabolism as quickly as possible through a snap freezing in liquid nitrogen. Afterward, depending on the technique and on the strategy employed until extraction or freeze-dried for longer storage, to avoid any water absorption, the plant tissue samples can be stored at -80ºC. The next crucial step is the extraction of the low molecular weight metabolites with a mixture of solvents or the use of either whole plants, organs such as leaves or roots, or parts of tissues. MS technique requires a pre-separation of the metabolic components using either GC after chemical derivatisation, or LC prior to analysis contrarily to the NMR spectroscopy that does not depend on an obligatory step for sample preparation (Schwender, 2009).

In metabonomics applications, MS provides both sensitive detection and metabolite identification but, it is destructive and the preparation of samples is more time consuming. NMR spectroscopy is a non-destructive technique and enables fast different metabolites identification and quantification. Although, the reduced sensitivity limits the observation to an estimated hundred or so metabolites per sample, this technique is an effective technique for metabolic profiling applications (Colquhoun, 2007).

The multivariate statistical methods use unsupervised methods, such as Principal Component Analysis (PCA) and supervised methods, such as Partial Least Squares (PLS) to visualize the complex multivariate data sets resulting from the metabolic profiling techniques (Lindon and Nicholson, 2008a).

1.3.2. NMR spectroscopy

Discovered in the 1950s, NMR spectroscopy has developed into a powerful, interdisciplinary method which delivers qualitative and quantitative information on a wide range of chemical species in a single experiment and provides detailed information on molecular structure, in pure compounds and in complex mixtures (Liu *et al.,* 1996; Nicholson *et al.,* 2002). Due to this, the high resolution ^{1}H NMR spectroscopy has been extensively used as an analytical tool to analyse metabolites in fruits and vegetables, such as mango (Duarte *et al.,* 2006), lettuce (Sobolev *et al.,* 2005), and tomato (Sobolev *et al.,* 2003).

1.3.2.1. Principles of NMR spectroscopy

In order to understand the basic principles of NMR spectroscopy it is necessary to comprehend the energy states, population distribution and relaxation phenomena. The energy difference between energy states gives rise to the frequency of spectra, while intensities of spectral peaks are proportional to the population differences of the states and relaxation phenomena occurrence influence both line shapes and intensities of NMR signals. The NMR spectroscopy technique is dependent on the magnetic properties of the atomic nucleus since nuclei with an even number of both charge and mass have a spin quantum of zero will not give NMR signals, called NMR inactive nuclei (Breitmaier, 2002; Jacobsen, 2007; Teng, 2005).

For nuclei with a non-zero spin quantum number, I≠0, such as ^{1}H and ^{13}C, energy states are produced by the nuclear angular moment, P, interacting with the applied magnetic field, B_0, which is governed by the Boltzmann distribution. These nuclei will rotate about the field direction due to the torque produced by the interaction of the nuclear angular momentum with the static magnetic field (Figure 1.4) (Lindon *et al.*, 2007).

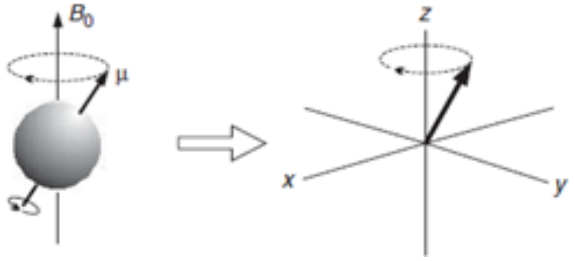

Figure 1.4: Precession of the nucleus as a result of a static magnetic field applied (Claridge, 2009).

The magnetic moment (or nuclear moment), μ, is either parallel or antiparallel to their angular momentum, given by $\mu = \gamma P$, in which γ is the nuclear gyromagnetic ratio, is a characteristic constant for a specific nucleus. For example, the proton has spin 1/2 so there are two possible orientations, either pointing up defined as the lower energy state, β, (I_z=1/2) or pointing down defined as higher energy state, α, ($I_z = -1/2$) (Figure 1.5) (Breitmaier, 2002).

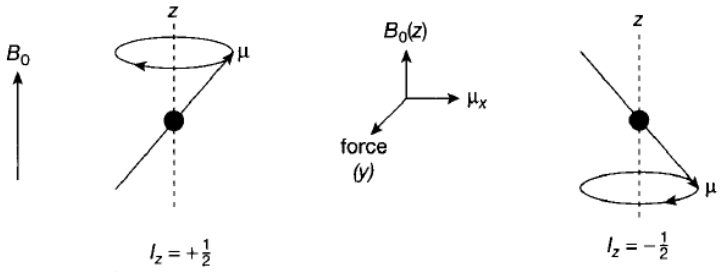

Figure 1.5: Orientation of nuclear angular moment, μ, with spin ½ and its z component and interaction between a spinning nucleus and an external field (Breitmaier, 2002).

The observable NMR signals come from the assembly of nuclear spins in the presence of the magnetic field. It is the bulk magnetization, M_0, of a sample that gives the observable magnetization, which is the vector sum of all spin moments (nuclear angular moments) and results from the small population between the lower and higher states (Figure 1.6) (Claridge, 2009).

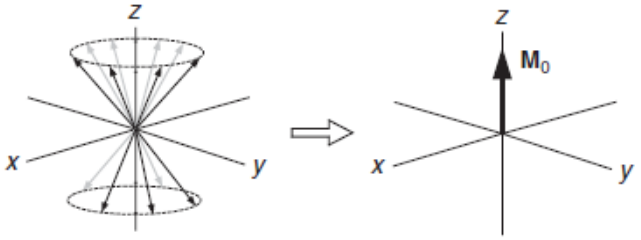

Figure 1.6: The bulk magnetization, M_0, at equilibrium (Claridge, 2009).

The nuclei are then excited by the radio frequency pulse during a defined period of time, and upon returning to equilibrium (relaxation) during acquisition time induce a signal which is detected as an NMR signal. The decay of the NMR signal with time produces the observed free induction decay. Performing a mathematical operation, the Fourier transformation, on the time-domain data a spectrum is generated giving intensity of signals as a function of frequency, that is to say a spectrum (illustrated in Figure 1.7) (Breitmaier, 2002; Jacobsen, 2007).

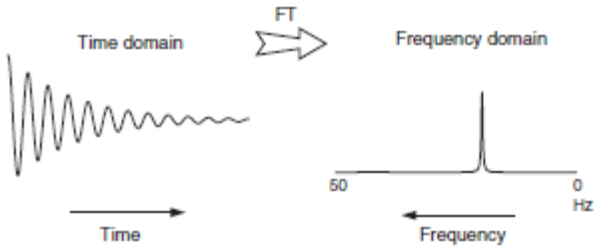

Figure 1.7: Fourier transformation (FT) of time domains free induction decay results in the corresponding frequency domain spectra (Claridge, 2009).

The subtle variation, that occurs because the bonding electrons create their own small magnetic field that modifies the external magnetic field in the surrounding area of the nucleus, is called chemical shift. The chemical shift is represented by the greek letter delta, δ, which gives detailed information about the structure of molecules and is given in parts per million (ppm). The frequency difference, in hertz (Hz), is measured from the resonance of a standard substance, typically Tetramethylsilane (TMS, 0 ppm) divided by the absolute value of the strength of the magnetic field and for ^{1}H NMR, the range of frequencies over which NMR signals are detected, is usually from 0-10 ppm (Claridge, 2009; Teng, 2005).

1.3.2.2. One-dimensional and two-dimensional NMR spectroscopy

The interpretation of ^{1}H NMR spectra requires one-dimensional (1D) and two-dimensional (2D) methods, and the comparison with libraries of reference compounds (Breitmaier, 2002; Teng, 2005).

1D NMR spectroscopy is used as a first screening method in metabonomics assignment studies, because this method has a rapid acquisition time of the samples analysed. Since material that have high content of water which can make unclear the spectrum acquired, it is necessary to remove the water signal by a water suppression sequence, such as simple presaturation, NOESYPRESAT or Watergate Sequences (Claridge, 2009).

The ^{1}H 1D NMR spectrum can be acquired through the use of three types of 1D experiment, namely, 1D pulse-and-acquire experiment, which capture information on every metabolite in one single analytical run, Carr-Purcell-Meiboom-Gill, and diffusion-edited experiments (Graça *et al.*, 2009; Lindon *et al.*, 2007).

In the 1D pulse-and-acquire experiment the small and large molecules are involved in the intensity of the signal which is proportional to their concentration and this experiment is usually used in metabonomics. However, one of the major disadvantages of this experiment is due to severe overlapping of the signals which disables the completely spectral assignment (Colquhoun, 2007).

2D NMR methods partially resolves this problem and improves the resolution of the spectrum, which helps identifying metabolites, because one second frequency dimension is introduced which disperses the signals over two-frequency dimensions. 2D experiments have always the same basic sequence which consists in a preparation (P), evolution (E), mixing (M) and detection periods (D) (Figure 1.8) and two frequency dimensions may represent any combination of chemical shifts or scalar couplings (Griffiths *et al.*, 2000; Lima *et al.*, 2010).

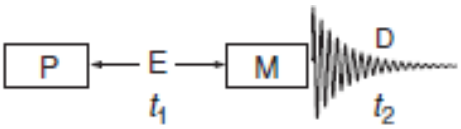

Figure 1.8: Common scheme in a 2D experiment (Claridge, 2009).

The COrrelation SpectroscopY (COSY) (Aue *et al.*, 1976) and TOtal Correlation SpectroscopY (TOCSY) (Braunschweiller *et al.*, 1983) are examples of 2D NMR experiments and both of them provide ^{1}H-^{1}H spin-spin coupling relations, in which the resonance frequency of one peak is related to those of its neighbours. As well, the ^{1}H-^{13}C correlation experiments, such as Heteronuclear Single-Quantum Correlation (HSQC) (Bodenhausen and Ruben, 1980) represent the 2D NMR experiments, in which the frequency axes display two different interactions (Breitmaier, 2002; Teng, 2005).

COSY (Figure 1.9) principal applications are the correlation of coupled homonuclear spins and correlation of protons coupled over two or three bonds (Claridge, 2009).

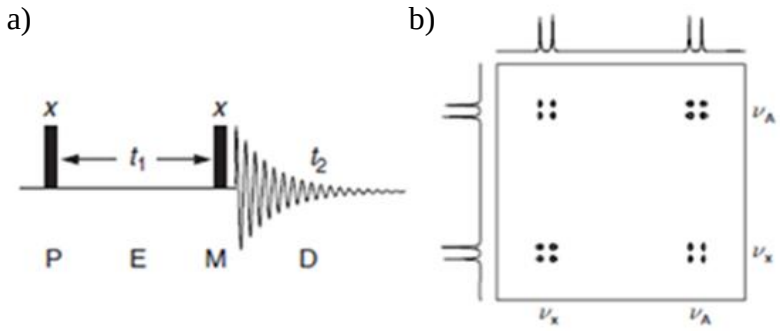

Figure 1.9: Illustration of a) basic COSY sequence and b) COSY spectrum of a coupled, two-spin AX system (Claridge, 2009).

TOCSY experiment is used for correlating coupled homonuclear spins and those that reside in the same spin system, and to employ the propagation of magnetization along a continuous chain of spins (Figure 1.10). This technique is most often applied in proton spectroscopy although it is equally applicable to any high-abundance nuclide. The major features of the TOCSY experiment are its high sensitivity, can overcome ambiguities arising from crosspeak overlap, and in-phase lineshapes can provide correlations even in the presence of broad resonances (Claridge, 2009).

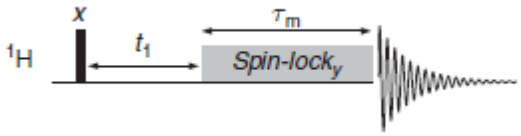

Figure 1.10: Illustration of a TOCSY sequence (Claridge, 2009).

The main applications of HSQC experiment are correlation of coupled heteronuclear spins across a single bond and identification of the directly connected nuclei. Moreover this technique employs detection of high-sensitivity nuclide, e.g. ^{19}F and provides better suited technique for crowded spectra although it may be more sensitive to experimental imperfections (Claridge, 2009).

In the Figure 1.11 an HSQC spectrum of lettuce water-soluble fraction is shown, that combined with other 2D sequences such as COSY and TOCSY, allowed to assign the peaks from the overlapped spectral region, i.e. the mid-field region (Sobolev et al., 2005).

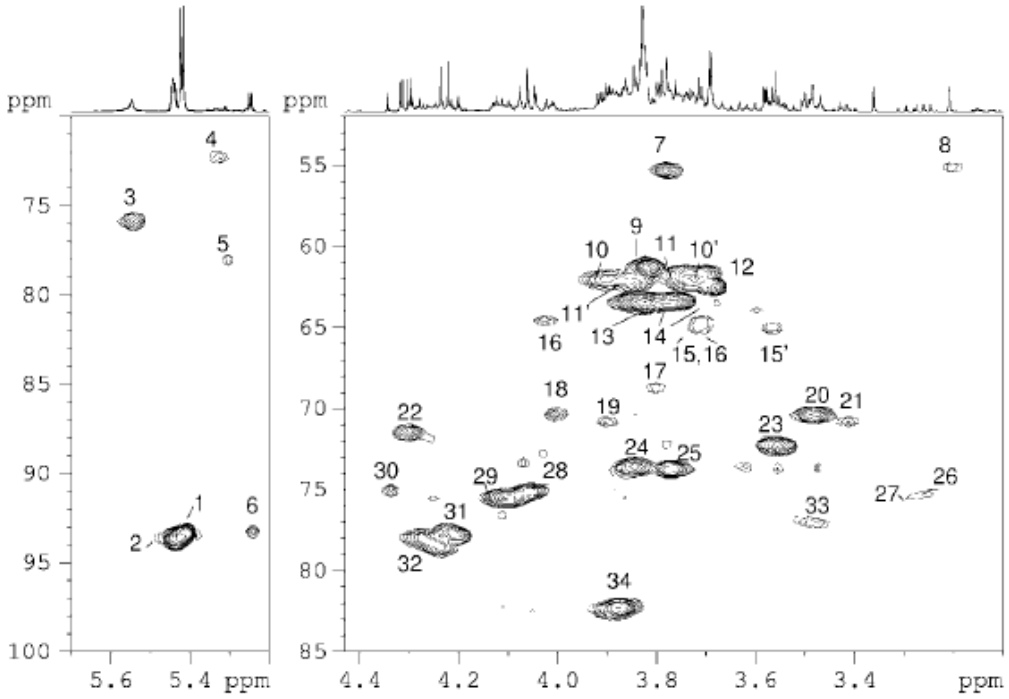

Figure 1.11: $^{1}H–^{13}C$ HSQC of lettuce water-soluble fraction, mid field and anomeric spectral regions (Sobolev *et al.*, 2005). *Key*: α-Glc, D-α-glucose; β-Glc, D-β-glucose; α-FF, D-α-fructofuranose; β -FF, D- β-fructofuranose; β -FP, D- β -fructopyranose; Suc, sucrose; Inul, inulins. *Assignments*: **1**- CH-1, Suc (Glc); **2**- CH-1, Inul (Glc); **3**- CH(O)COOH, Chicoric A.; **4**- CH-3, Chlorogenic A.; **5**- CH(O)COOH, Monocaffeoyltartaric A.; **6**- CH-1 α-Glc; 7- α-CH, Gln and Glu; **8**-$N(CH_3)_3$ choline; **9**- CH_2-6, Suc, Inul; **10** and **10**'- CH_2-6 β-Glc; **11**, and **11**'- CH_2-6 α-Glc; **12**- CH-1', Suc, Inul; **13**- CH_2-6', Suc, Inul; **14**- CH_2-6 β-FF; **15** and **15**'- CH_2-1 β-FP; **16** and **16**'- CH_2-6 β-FP; **17**- CH-3 β-FP; **18**- CH-5 β-FP; **19**- CH-4 β-FP; **20**- CH-4 Suc, Inul; **21**- CH-4 α- and -β-Glc; **22**- α-CH malate; **23**- CH-2 α-Glc and Suc, Inul; **24**- CH-5 Suc, Inul; **25**- CH-3 Suc, Inul; **26**- CH-2 β-Glc; **27**- CH-4 *myo*-inositol; **28**- CH- 4' Suc, Inul; **29**- CH-4 β-FF, CH- 4' Inul; **30**- α-CH tartrate; **31**- CH- 3' Suc, Inul; **32**- CH- 3' Inul; **33**- CH-3 and CH-5 β-Glc; **34**, CH- 50 Suc, Inul.

1.3.2.3. Magic angle spinning NMR

The Magic Angle Spinning (MAS) technique has developed for solid state NMR spectroscopy (Teng, 2005). The experimental focus of the MAS technique consists on inserting the sample in a rotor (Figure 1.12 a), followed by a rapid spinning, of the sample

about the direction along the magic angle, 54.74º, (Figure 1.12 b) at a rate larger than the anisotropic line width, relative to the applied magnetic field, B_0 (Lindon *et al.,* 2009).

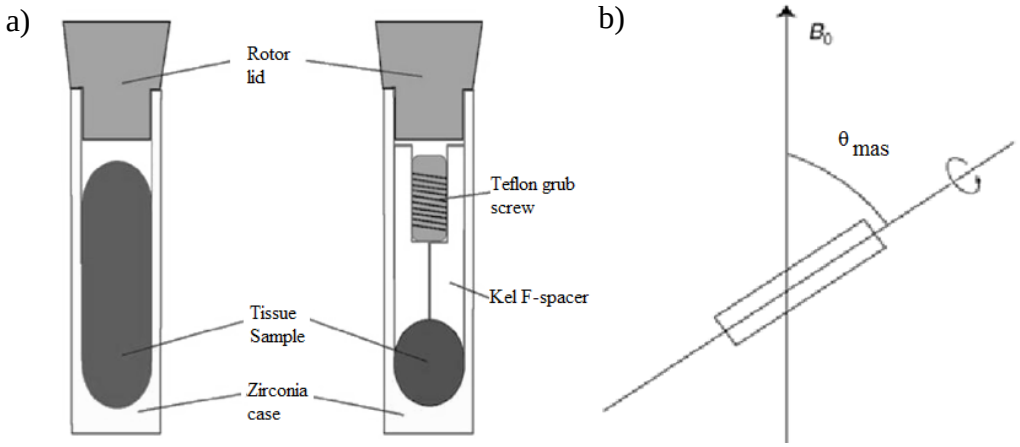

Figure 1.12: Illustration of a) a zirconia 4 mm o.d. rotor with Kel-F spacers for spherical sample volume and b) magic angle sample spinning. Adapted from Claridge (2009) and Lindon *et al.* (2009).

Figure 1.12 a display the most commonly used rotors for MAS which are made of zirconium oxide (zirconia), in the left is represented the 4 mm rotor that can be entirely filled with sample. In the right it is display the rotor normally used in High Resolution MAS (HRMAS) NMR spectroscopy, with a spherical insert and Kel F-spacer. The rotor spacer reduces the volume of sample on the rotor, but the homogeneity and spectral quality are improved.

The disposition of the sample in MAS makes possible to simulate the effect of molecular tumbling in solution state, which reduces the line-broadening of chemical anisotropy and dipolar interactions, seen in non-liquid samples, reducing the loss of information (Figure 1.13 a and b). Moreover, the spectral resolution in semi-solid samples may be enhanced throughout the use of a high resolution probe coupled with MAS (Figure 1.13 c) (Weybright *et al.*, 1998).

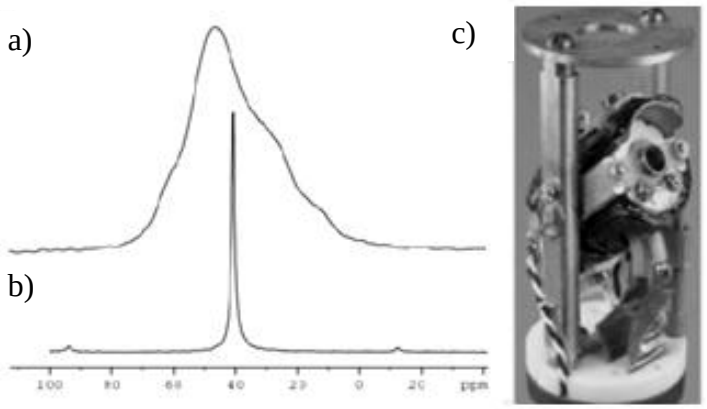

Figure 1.13: Illustration of a) ^{1}H decoupled ^{13}C powder pattern, b) magic angle spinning spectra of $^{13}C_2$ Glycine and c) a high resolution probe coupled with MAS (HRMAS) NMR probe for a 4 mm rotor sample, showing a gradient coil at the magic (Lindon *et al.*, 2007; Teng, 2005).

The HRMAS NMR spectroscopy has been used in the study of the metabolome of foodstuff, because it allows the measuring of samples without any chemical and/or physical preparation by means of highly resolved NMR spectra. The work hereby reported, uses the ^{1}H HRMAS NMR spectroscopy and below, some studies that used this technique, are given as examples.

Ritota *et al.* (2010) characterized sweet pepper (*Capsicum annum* L.) of different cultivars by HRMAS-NMR spectroscopy combined with multivariate analysis. For 1D spectra fresh pepper was used and for 2D spectra the samples were frozen in liquid nitrogen and powdered in a ceramic mortar with a pestle (smashed) at a spinning rate of 7 kilohertz (kHz). In a single experiment it was possible to observe organic acids, fatty acids, amino acids, and some minor compounds without any extraction, purification and separation steps. In addition, taking together the results of HRMAS NMR and statistical models allow the discrimination of peppers from different cultivars

Pérez *et al*. (2010) studied the suitability of ^{1}H HRMAS NMR as an efficient technique for metabolic profiling of tomatoes ripening (green, turning and red) and for metabolic profiling of mature red tomatoes flesh, peel and seeds from mature red fruits. The NMR data were obtained from ^{1}H-HRMAS-NMR spectra of tomato purée, followed by the chemometric methods. The major components found in the spectra of flesh, peel and tomato purée were fructose, glucose, citric acid, and the amino acids GABA, glutamine

and glutamate. The chemometric methods allowed a clear separation between peel and flesh and to visualize the metabolic trajectory from green to red mature stages.

1.4. Objectives of this work

This study aimed to determine the metabolic profile of lettuce leaves by ^{1}H HRMAS NMR spectroscopy. In addition, through the use of the lettuce as a model in toxicology tests assess changes on the metabolic and physiological response of lettuce leaves due to aging, to differences in light growth conditions and to mancozeb exposure. Moreover, since pH and ionic strength can cause variations in the chemical shifts and on the intensities of the metabolites, the influence of disodium ethylenediaminetetraacetic acid (EDTA) to lettuce leaves on ^{1}H HRMAS NMR spectra was also study.

2. Experimental Section

2.1. Plant Material and Lettuce Culture Conditions

Seeds of *Lactuca sativa L.* (var. May Queen), from Viveiros Litoral, were germinated in water and then transferred to plastic pots with a mixture of turf and vermiculite (2:1). Cultures were maintained in a growth chamber with a temperature of 20 ± 2°C, a 16/8-h (day/night) photoperiod with a photosynthetic photon flux density of app. 200 ± 20 µmol m^{-2} s^{-1}. Four week old plants were randomly separated in two groups:

A- Growth conditions for EDTA, light growth conditions, and aging studies

Two different light intensities were applied: a) *light conditions* - a group of plants was maintained under growth chamber conditions with a light intensity of app. 200 ± 20 µmol.m^{-2}.s^{-1} (control), and b) *dark conditions* - a group of plants was maintained under growth chamber conditions but with a light intensity of app. 20 ± 20 µmol.m^{-2}.s^{-1}. After 7 days, pigments content and photosynthetic efficiency measurements were performed with a Mini-Pam fluorometer (Walz, Germany). Simultaneously, leaf samples were taken and frozen in liquid nitrogen. For the conditions on study the leaves from the first (expanded leaves) and apical nodes (young leaves) were collected (Figure 2.1 I and II respectively). Samples were maintained at -80ºC until NMR analysis.

B- Growths conditions for mancozeb studies

Four week old plants were sprayed with mancozeb (PESTANAL®, analytical standard, Sigma) (6.2 mg/L). Another group of plant, designated as control plants, was maintained under the same growth conditions but not exposed to mancozeb. Cultures were maintained in a growth chamber with a temperature of 20 ± 2°C, a 16/8-h (day/night) photoperiod with a photosynthetic photon flux density of app. 200 ± 20 µmol.m^{-2}.s^{-1}. After 7 days of mancozeb exposure, pigments content and photosynthetic efficiency measurements were performed in exposed and control plants with a Mini-Pam fluorometer (Walz, Germany). Simultaneously, leaf samples were taken and frozen in liquid nitrogen. Samples were maintained at -80ºC until NMR analysis.

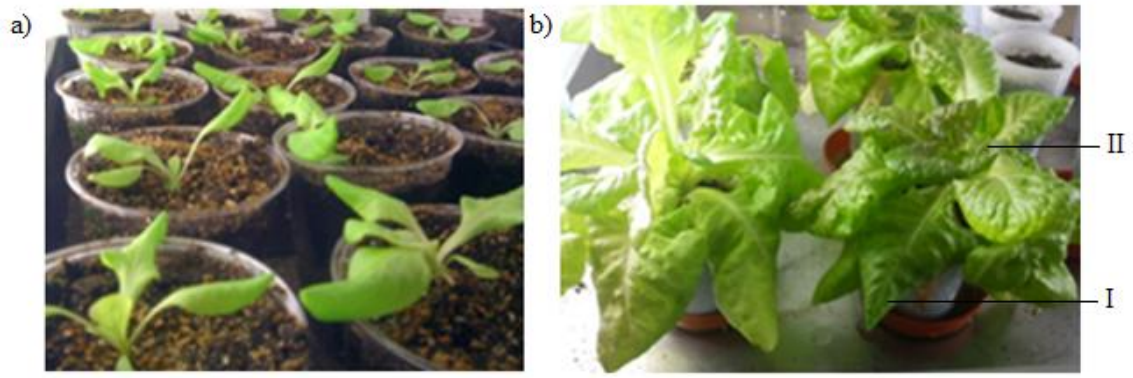

Figure 2.1: Lettuce plants growing in a growth chamber, a) one week old plants and b) four week old plants exposed to mancozeb. I) expanded leaves from the first node and II) young leaves from the apical node.

2.2. NMR Analysis

2.2.1. Sample preparation

For ^{1}H HRMAS NMR spectroscopy, the lettuce leaves were ground in a mortar to a powder, i.e. pooled material. From the pool were collected replicates, each of them 195 mg, to an eppendorf tube.

For studies in light growth conditions, aging and mancozeb effects, the replicates were mixed in an eppendorf tube with 250 µL of a D_2O solution of 1 M phosphate buffer (61 mg NaH_2PO_4 and 82 mg of Na_2HPO_4 in 1 mL of D_2O), for stabilizing the pH at 6.70, and 1 mM sodium (trimethyl)propionic acid-2,2,3,3-d4 (TSP) as an internal reference. 50 µL of this mixture were then packed into a 4 mm MAS rotor.

For studies of EDTA effects, the same protocol was followed but 1 mM EDTA was added to the D_2O solution of 1 M phosphate buffer with TSP (Pérez *et al.*, 2010, Sobolev *et al.*, 2010).

2.2.2. NMR measurements

For EDTA, light growth conditions, and aging studies

HRMAS NMR spectra of lettuce leaves to study the effect of EDTA, light growth conditions and aging were recorded on a Bruker Advance spectrometer operating at 500 MHz for proton observation, at 277 k, equipped with a 4 mm HRMAS probe head, spinning the samples at the magic angle and at 4 kHz. ^{1}H HRMAS NMR spectra were acquired by using a water suppression pulse sequence, noesypr1d (Bruker library), using 32 K data points over a 6510 Hz spectral width and adding 256 scans.

For mancozeb studies

HRMAS NMR spectra of lettuce leaves to study the effect of mancozeb were recorded on a Bruker Advance spectrometer operating at 800 MHz for proton observation, at 277 k, using a 4 mm HRMAS probe, in which the rotor containing the sample was spun at the magic angle and a 4 kHz spinning rate.^{1}H HRMAS NMR spectra were acquired by using a water suppression pulse sequence, noesypr1d (Bruker library), using 32 K data points over a 9803 Hz spectral width and adding 256 scans.

All ^{1}H NMR spectra were reference to the methyl groups signal at δ 0.00 ppm of TSP. Each spectrum was processed with a line broadening of 0.3Hz and a zero filling factor of 2, manually phased and baseline corrected.

2D homonuclear and heteronuclear spectra were registered for selected samples to aid spectral assignment. These included TOCSY and HSQC. Spectral assignment was carried out with the support of Bruker Biorefcode spectral database and with literature data. In Figure 2.2 presents a ^{1}H HRMAS NMR spectrum of young leaves recorder on Bruker Advance spectrometer operating at 500 MHz and 800 MHz respectively. As shown, it is clearly noticeable a greater sensitivity and less overlap in the spectrum acquired at 800 MHz.

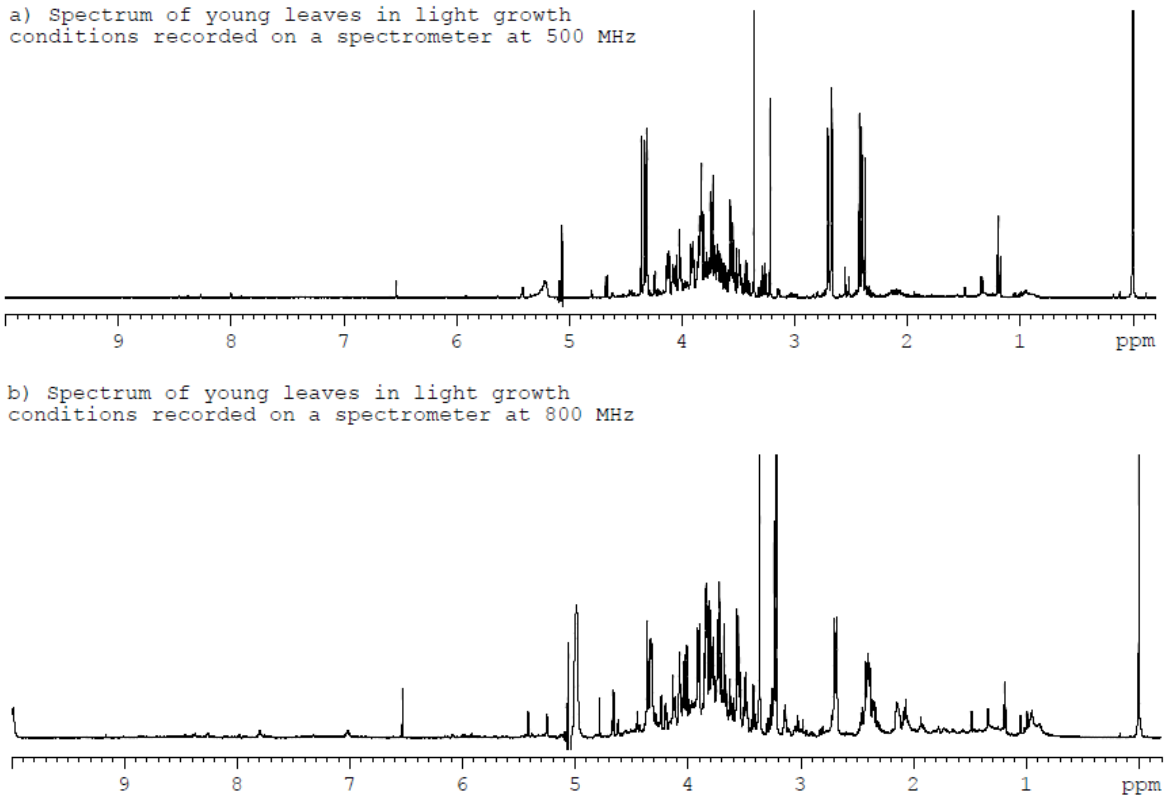

Figure 2.2: ^{1}H HRMAS NMR spectrum of young leaves recorder on Bruker Advance spectrometer operating at a) 500 MHz and B) 800 MHz.

2.2.3. Data analysis

Aiming to evaluate the variations of some metabolites, selected signals in the 1D spectra were integrated using the Amix-Viewer software (Bruker, version 3.9). Each area was normalized to total spectral area, excluding the water region, to allow comparison between samples. This method has some limitations because variation in metabolite absolute quantities may be hidden. Nonetheless, it still enables reliable intersample comparison in terms of relative amounts of compounds. The t-student test for the ^{1}H NMR signals was performed by R (version 2.9.2).

2.3. Pigments Content and Photosynthetic Efficiency Measurements

2.3.1. Quantification of pigments content

Leaves were ground in a mortal to a powder in 2 ml cold acetone/Tris 50 mM pH 7.8 buffer solution (80:20, v/v) and centrifuged at 28000rpm during 5 minutes. The supernatant was diluted to a final volume of 3 ml with additional acetone/Tris buffer according to Sims and Gamon (2002) method.

The absorbance at 470, 537, 647 and 663 nm were determined with a Thermo Fisher Scientific spectrophotometer (Genesys 10-uv S). The contents of Chl *a*, Chl *b* and carotenoids were calculated using the formulae of Sims and Gamon (2002).

2.3.2. Chlorophyll *a* fluorescence measurement

Chlorophyll *a* fluorescence measurements were performed *in situ* in full expanded leaves and in young leaves of lettuce with a portable fluorimeter Mini-Pam (Walz, Germany). Minimal fluorescence (F_0) was measured in 30 minutes dark-adapted leaves by applying a weak modulated light and maximal fluorescence (Fm) was measured after a 1 second saturating pulse of white light (>1500 μmol m^{-2} s^{-1}) in the same leaves. In light adapted leaves, steady state fluorescence (F_s), maximal fluorescence (F´m) after 1 s saturating pulse (>1500 mol m^{-2} s^{-1}) and minimal fluorescence (F'_0) measured when actinic light was turned off, were determined. Definitions of fluorescence parameters (F_v/F_m and Φ_{PSII}) were used as described by van Kooten and Snel (1990) in which Φ_{PSII} represents the number of electrons transported by a PSII reaction center per mole of quanta absorbed by PSII and F_v/F_m is the ratio of variable to maximal fluorescence.

2.3.3. Data analyses and statistics

Pigments content and chlorophyll fluorescence data were analyzed using a t-student test and when necessary data were transformed to achieve normality and equality of variance. When these criteria were not satisfied even with transformed data, the non-parametric Mann–

Whitney rank sum test was performed. All statistical analysis was performed using SigmaStat for Windows, version 3.1.

3. Results and Discussion

3.1. ^{1}H HRMAS NMR Spectroscopy Study of Lettuce Leaves

3.1.1. Spectral assignment

The ^{1}H HRMAS NMR spectrum of young lettuce leaves exposed to light growth conditions is given as example of a lettuce spectrum in Figure 3.1, the spectra display in this is expressed as mean of three replicates. Sobolev *et al.* (2005) published for the first time a detailed assignment of high resolution ^{1}H NMR spectra of lyophilized lettuce leaves. Contrarily to the authors, the Figure 3.1 show a spectra of powder lettuce leaves without lyophilization. The major difference between the spectra presented and the spectra obtained by these authors seems to be in the phenolic region, where they were able to indentify several phenolic compounds. Moreover, in Figure 3.1., the high-field region (0-3 ppm), the mid-field region (3-5.5 ppm) and low field region (5.5-10 ppm) are vertically expanded.

As it can be seen in the ^{1}H HRMAS NMR spectrum (Figure 3.1), the high-field region (0.0-3.0 ppm) presents signals arising from organic acids and amino acids, namely lactic acid, acetic acid, succinic acid, and fumaric acid. Citric and malic acid the two most predominant organic acids in lettuce (Sobolev *et al.*, 2005) are also shown in the spectrum. Several amino acids are detected in lettuce leaves, such as alanine, valine, threonine, and isoleucine. The ethanol was also identified in this region, supposedly deriving from fermentation processes or due to some type of contamination prior to NMR measurements.

In the mid-field region from 3.0 to 5.5 ppm there is an overlapping of peaks belonging to carbohydrates signals, such as β-glucose, α- glucose, fructose and sucrose. It is also possible to identify in this region the choline. Sobolev *et al.* (2005), also show that the major carbohydrates in the ^{1}H NMR spectrum of lyophilized lettuce were these sugars.

The weakest signals in the spectrum are presented in low-field region. The fumaric acid and formic acid signals were identified in the spectrum. Contrarily, to the work of Sobolev *et al.* (2005), in the ^{1}H NMR spectrum of lettuce the phenolic compounds were not assigned, but there are some signals that show no correlations in TOCSY making difficult to identify them. On the other hand, the total amount of phenolic compounds in leaves lettuce depends on the cultivar, on the ripening progress and postharvest storage conditions (Romani et al., 2002).

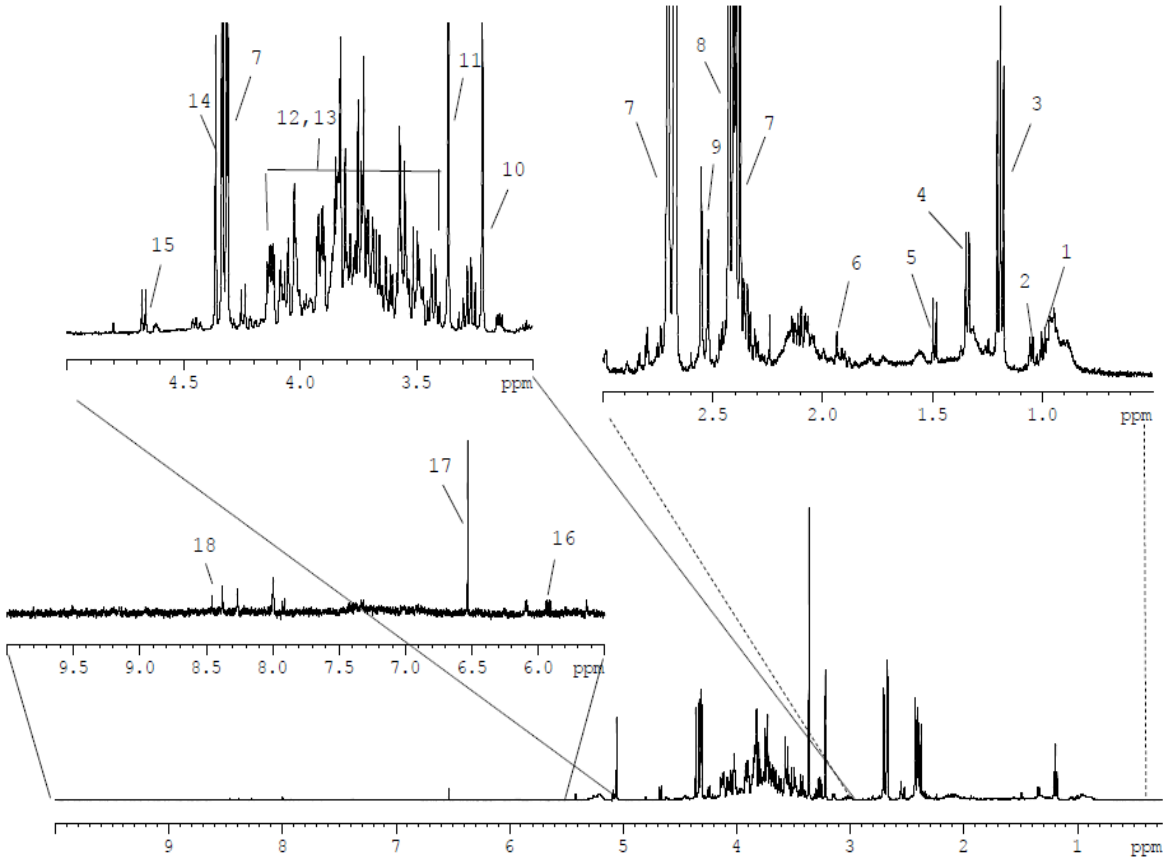

Figure 3.1: 500 MHz ^{1}H HRMAS NMR average spectrum of three replicates of young lettuce leaves exposed to light growth conditions measured at 277 K. Assignments: 1- valine; 2- isoleucine; 3- ethanol; 4- lactic acid; 5- alanine; 6- acetic acid; 7- malic acid; 8- succinic acid; 9- citric acid; 10- choline; 11- methanol 12, 13- glucose and fructose; 14- tartaric acid; 15- β-glucose; 16- uridine; 17- fumaric acid; 18- formic acid. The insets show expansions of the high-field, mid-field and low-field region.

In order to fulfill a detailed assignment of the metabolites present in lettuce leaves, some 2D experiments (TOCSY and ^{1}H-^{13}C HSQC) were used and, as well, the literature chemical shift data from other vegetables. Figure 3.2 showed the TOCSY spectrum of lettuce leaves, performed by us. A summary of the assignments from expanded and young lettuce leaves obtained, with chemical shifts and spin-spin coupling patterns (multiplicity) of metabolites is reported in table 3.1.

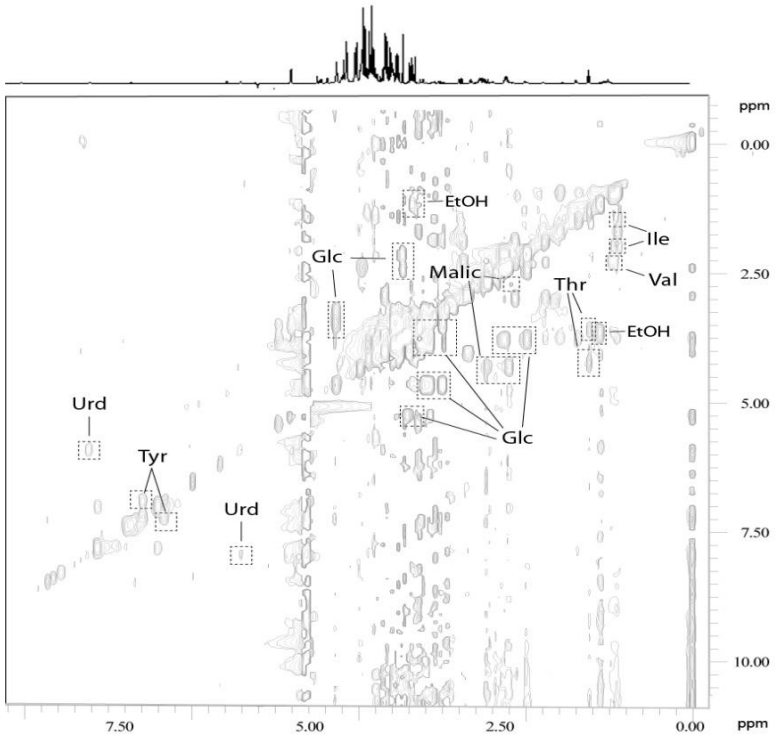

Figure 3.2: 500 MHz ^{1}H-^{1}H TOCSY of commercial lettuce leaves measured at 277 K. Abbreviations: Glc- glucose; EtOH- ethanol; Thr- threonine; Val- valine; Ile- isoleucine; Urd- uridine; Tyr- tyrosine.

Table 3.1: 500 MHz ^{1}H HRMAS NMR assignments for young lettuce leaves, and pH around 6.7. Abbreviations: s: singlet, d: doublet, t: triplet, q: quartet, dd: doublet of doublets, m: multiplet.

Compound	Assignment	δ (ppm)	Multiplicity
Valine	γ-CH_3	1.00	d
	γ'-CH_3	1.04	d
	β-CH	2.28	m
Ethanol	CH_3	1.17	t
	CH_2	3.63	
Alanine	α-CH	1.48	d
	β-CH_3	3.79	
Acetic acid	α-CH_3	1.94	s
Lactic acid	β-CH_3	1.32	d

Table 3.1 (Continued)

Compound	Assignment	δ (ppm)	Multiplicity
Malic acid	α-CH	2.38	dd
	β'-CH	2.67	dd
	β-CH	4.30	dd
Succinic acid	α, β-CH_2	2.42	s
Citric acid	αγ-CH	2.52	d
Choline	$N(CH_3)^{3+}$	3.22	s
β-Glucose	CH-1	4.66	s
	CH-2	3.25	dd
	CH-3	3.53	t
	CH-4	3.40	dd
	CH-5	3.45	
	CH_2-6,6'	3.88; 3.75	
α-Glucose	CH-1	5.26	d
	CH-2	3.55	
	CH-3	3.73	
	CH-4	3.41	d
			dd
Fumaric acid	α,β-CH=CH	6.54	s
Formic acid	HCOOH	8.46	s
Threonine	γ-CH_3	1.34	d
	α-CH	3.60	
Sucrose	CH-1 (Glc)	5.40	d
	CH-2	3.57	
	CH-3’	4.22	d
Isoleucine	γ-CH3	1.02	d
	γ’-CH	1.47	t
Methanol	CH_3	3.36	s
Tartaric acid	CH(OH)COOH	4.34	s
Fructose	CH-3	4.12	m
	CH-4	4.12	m

Table 3.1 (Continued)

Compound	Assignment	δ (ppm)	Multiplicity
Tartaric acid	CH(OH)COOH	4.34	s
Fructose	CH-3	4.12	m
	CH-4	4.12	m
Tyrosine	CH-3, CH-5 ring	6.90	d
	CH-2, CH-6 ring	7.19	d
Uridine	CH-1’	5.89	
	CH-6 ring	7.85	d

3.2. Study of the Effects of Addition of EDTA

The ^{1}H HRMAS NMR spectrum of lettuce contains a large number of detectable metabolites, and is, therefore, highly suitable for the study of perturbations caused by xenobiotics and other environmental factors. However, the pH and ionic strength can cause variations in the chemical shifts and on the intensities of these metabolites (Asiago *et al.*, 2008). Therefore, in such studies it is important to distinguish between the physiological response and biological/technical variation. EDTA as a chelate that binds to many metal ions establishes stable complexes with them, which minimizes the frequency shifts of these metabolites. Chelation of such metal ions is evident due to appearance of signals from EDTA complex to divalent metal ions such as calcium and magnesium (Han and Ba, 2004; Han *et al.*, 2007). The combination of EDTA and an appropriate buffer effectively minimizes both dependent frequency shifts and ionic strength dependent intensity variations, and it has been used in NMR based applications for metabonomics approaches by Pérez *et al.* (2010) and Sobolev *et al.* (2010). Therefore, with a view towards understanding and minimizing the effects of these variations the EDTA was added during sample preparation, in young and expanded lettuce leaves exposed to light and dark growth conditions.

3.2.1. Effects of the addition of EDTA to young lettuce leaves

In light growth conditions

In Figure 3.3 is presented the spectrum of young leaves without addition of EDTA during sample preparation and with addition of EDTA during sample preparation, a and b respectively. The two spectrum compared show that the use of EDTA seems to result in a trend of narrower peaks (indicated with arrows in Figure 3.3 b).

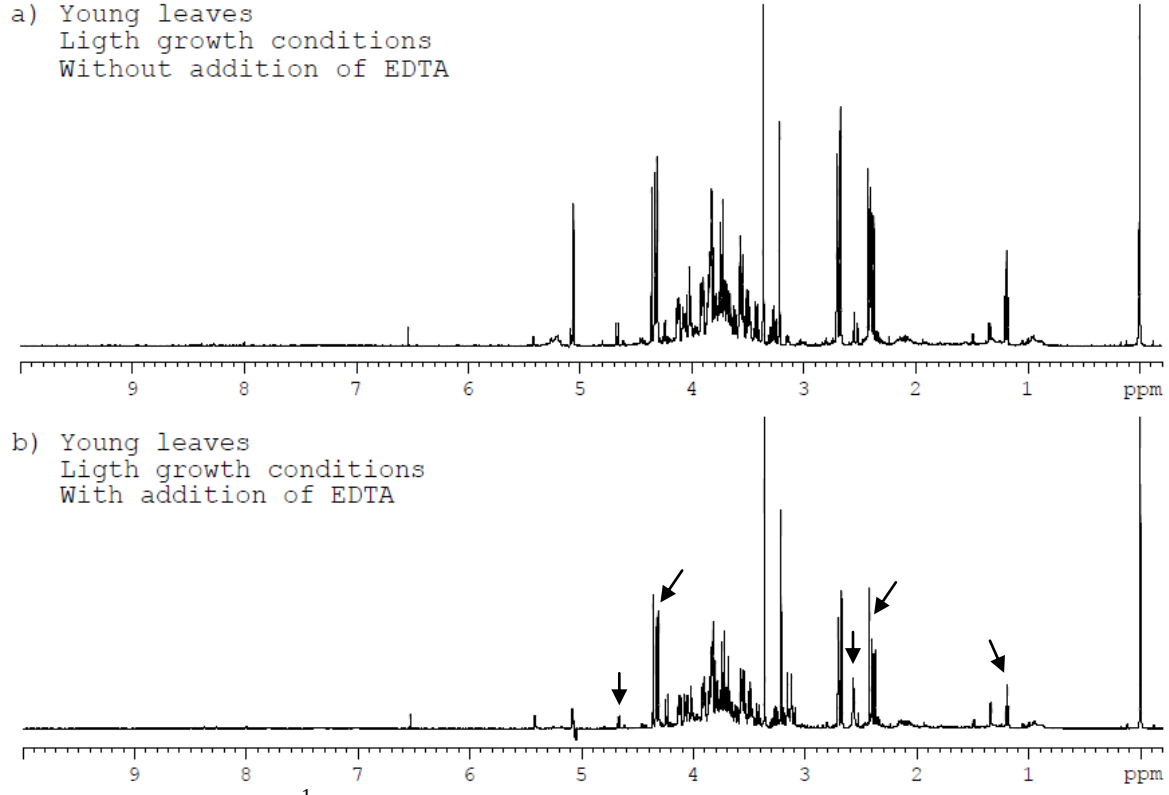

Figure 3.3: 500 MHz ^{1}H HRMAS NMR average spectrum of three replicates of young lettuce leaves exposed to light growth conditions, measured at 277 K, a) without addition of EDTA and b) with addition of EDTA during sample preparation. Arrows indicate signals undergoing significant changes.

Figure 3.4 b shows an increase on the resolution of the lactic acid signal (indicated with arrows), comparatively to the same signal arising from the sample without addition of EDTA (Figure 3.4 a). In addition, the malic acid, at 2.38 and 2.67 ppm, and succinic acid, at 2.42 ppm, also show a narrow NMR signals, resulting in a more resolved signals. The line broadening in the presence of metal ions, namely magnesium (Mg^{2+}) and calcium

(Ca^{2+}), arises from the chemical exchange between the metabolite bound to the metal ion and the corresponding metabolite in its free form, which have slightly different chemical shifts. For these reasons, when the metal ions are chelated by EDTA, such metabolites exist essentially in the free form (unbound) resulting in narrower NMR signals (Asagio *et al.*, 2008).

The binding of EDTA with the divalent metal ions in lettuce results in the appearance of characteristic NMR signals due to the formation of Ca-$EDTA^{2-}$ and Mg-$EDTA^{2-}$ complexes (Barton *et al.*, 2009). A recent NMR study on EDTA-complexation has shown that EDTA binds with Ca^{2+} and Mg^{2+} ions under physiological conditions (Somashekar *et al.*, 2006). Contrarily, to the results presented by Somashekar *et al.* (2006), the spectrum of young leaves with addition of EDTA (Figure 3.4), did not present the formation of the Mg-$EDTA^{2-}$ complex, by the appearance of characteristic signals at 2.72 and 3.23 ppm but presented the formation of the Ca-$EDTA^{2-}$ complex. The Ca-$EDTA^{2-}$ complex present an AB pattern comprising of chemical shifts at 3.09 ppm and a single line at 2.56 ppm, for the acetate-methlylene protons and backbone-methylene protons with quartet and singlet multiplicity respectively (Han and Ba, 2004). In the Figure 3.4 b, it appears the characteristic NMR signal at 2.56 ppm and in Figure 3.5 b at 3.09 ppm due to the formation of a Ca-$EDTA^{2-}$ complex.

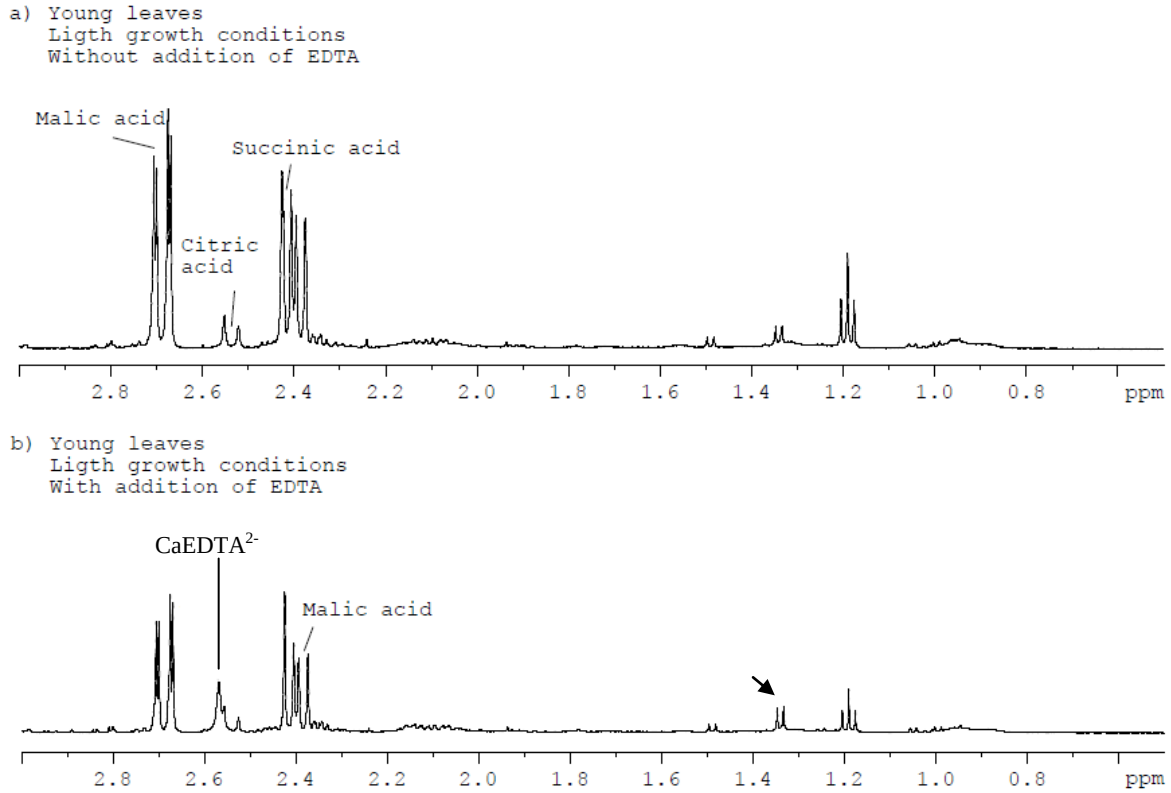

Figure 3.4: High-field region of the 500 MHz ^{1}H HRMAS NMR average spectrum of three replicates of young lettuce leaves exposed to light growth conditions, measured at 277 K., a) without addition of EDTA and b) with addition of EDTA during sample preparation. Arrow indicates signal undergoing significant variation.

The mid-field region (3 to 5.5 ppm) is dominated by intense and overlapped signals of the major sugars present in the lettuce, such as glucose, fructose and sucrose (Figure 3.5 b). The use of EDTA seems to increase the resolution of their signals, because the signals of sucrose at 4.22 ppm and fructose at 4.12 ppm are more narrow and intense as a result of the use of EDTA as shown in Figure 3.5 b (indicated with arrows).

Similarly, the line width of the tartaric acid and malic acid peaks is reduced upon addition EDTA, resulting in narrower NMR signals.

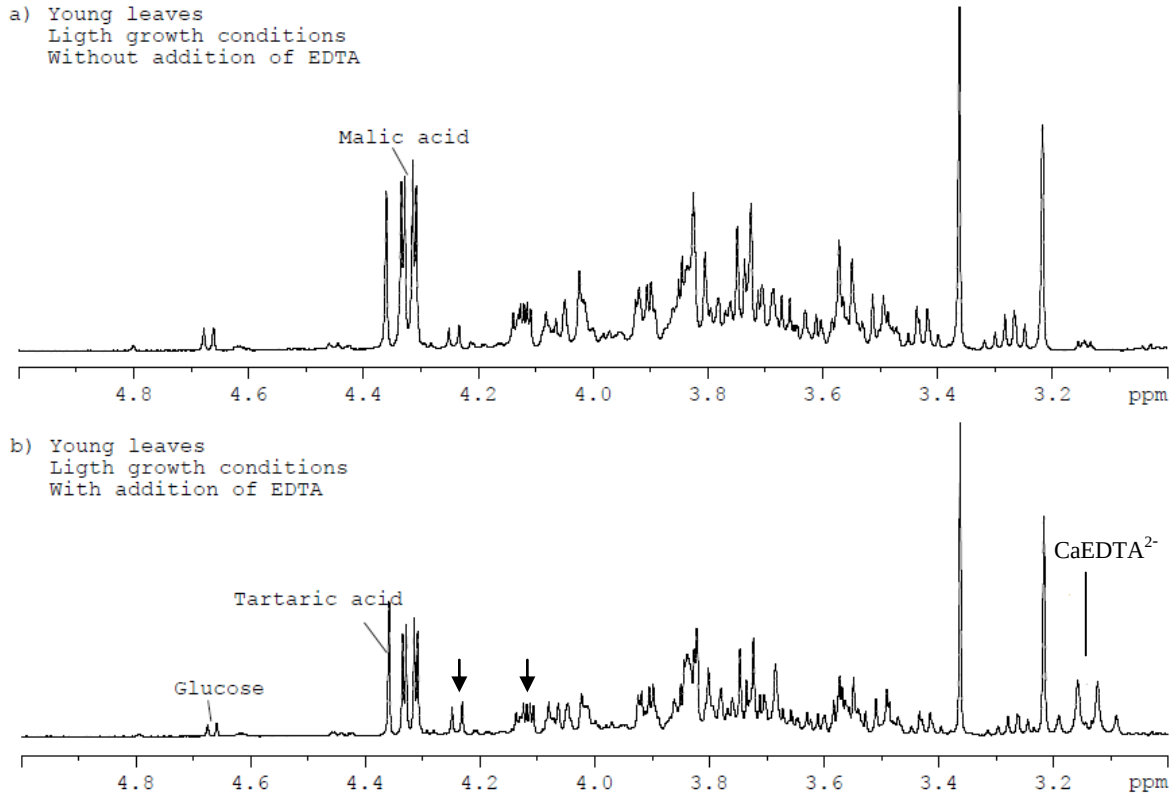

Figure 3.5: Mid-field region of the 500 MHz ^{1}H HRMAS NMR average spectrum of three replicates of young lettuce leaves exposed to light growth conditions, measured at 277 K., a) without addition of EDTA and b) with addition of EDTA during sample preparation. Arrows indicate signals undergoing significant changes.

The signals that arise in the low-field region (5.5-10 ppm) are the weakest in the spectrum. In Figure 3.6 b the addition of EDTA improves the peak width by reducing the interaction of divalent metal ions, namely calcium, with the sucrose at 5.40 ppm and some unassigned metabolites from 7.9 to 8.4 ppm in the young leaves lettuce NMR spectrum.

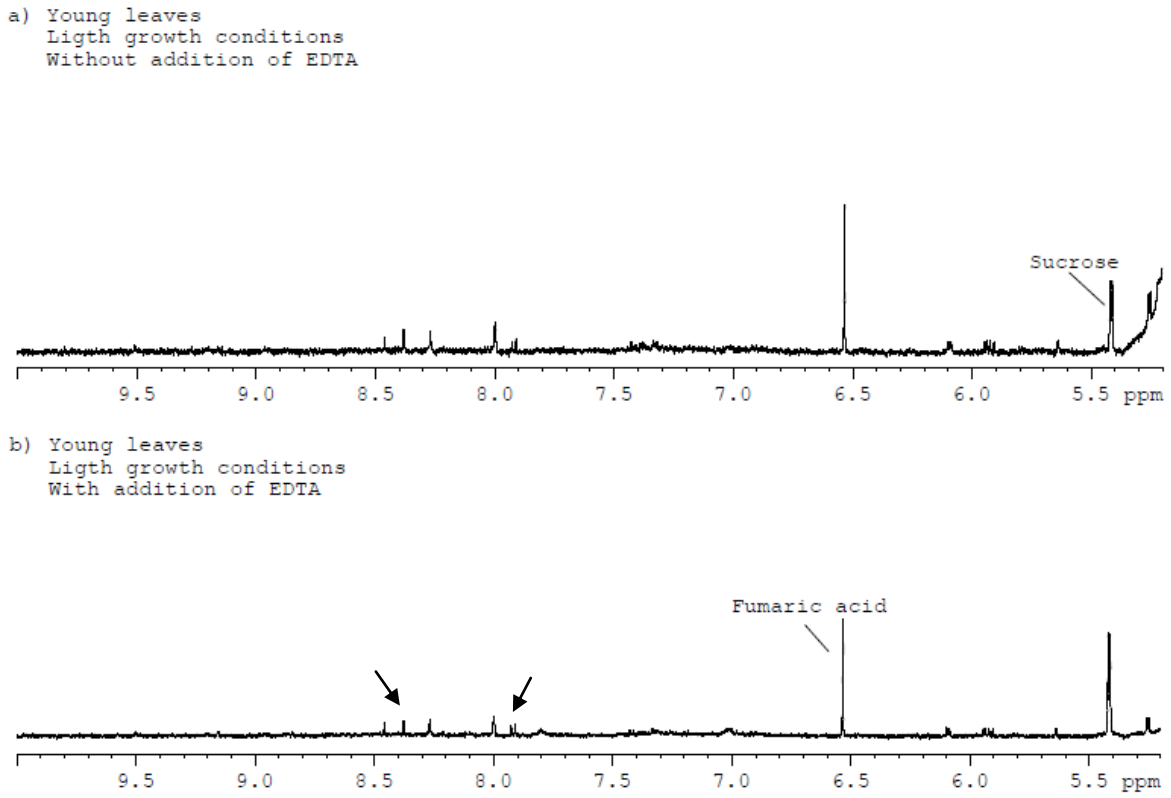

Figure 3.6: Low-field region of the 500 MHz ^{1}H HRMAS NMR average spectrum of three replicates of young lettuce leaves exposed to light growth conditions, measured at 277 K., a) without addition of EDTA and b) with addition of EDTA during sample preparation. Arrows indicate signals undergoing significant changes.

In dark growth conditions

Figure 3.7 shows the comparison between young leaves without addition of EDTA (Figure 3.7 a) and the same leaves with EDTA addition (Figure 3.7 b), grown in dark conditions. As can be seen, in Figure 3.7 b, the EDTA greatly affects the shape of ^{1}H NMR signals, enabling a higher resolution of the spectrum, which implies that peaks are narrower and more intense (indicated with arrows). However, the use of EDTA also results in the addition of some signals to the spectrum, in the high-field region (0-3 ppm) and low-field region (5.5-10 ppm), which makes the information interpretation and retrieval more difficult in these regions (indicated with arrows in Figure 3.7).

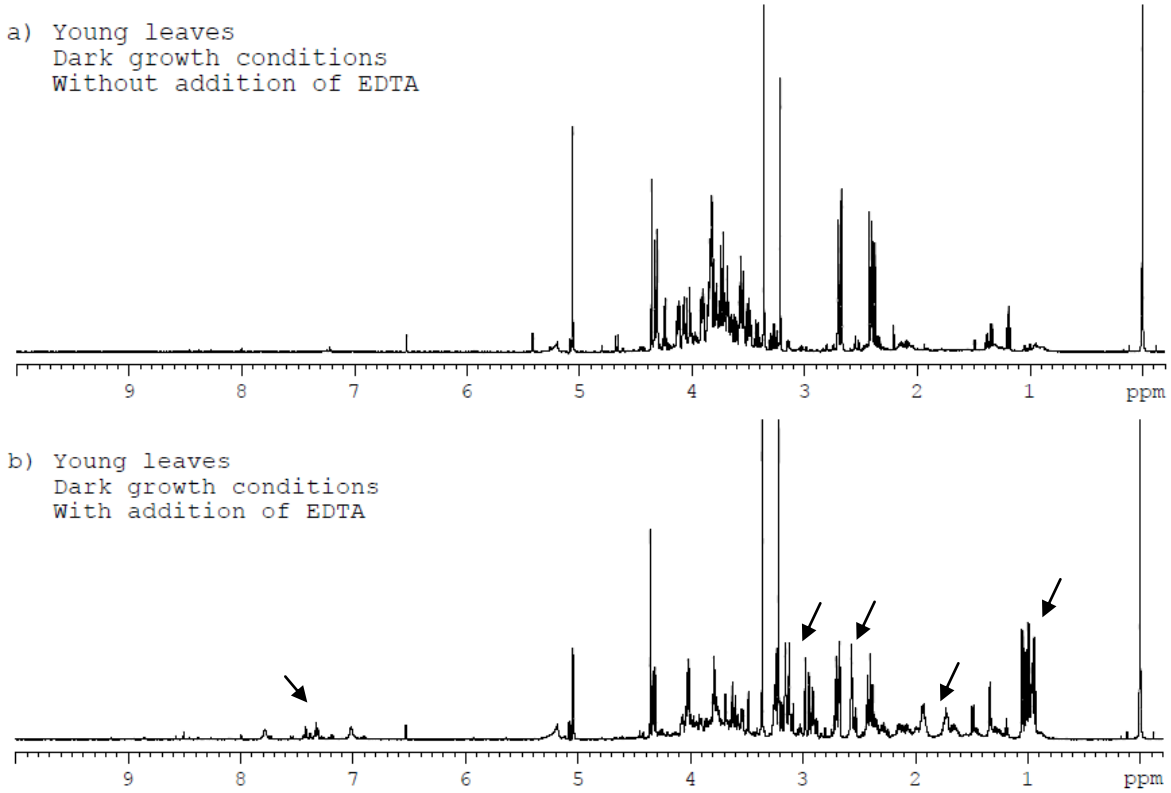

Figure 3.7: 500 MHz ^{1}H HRMAS NMR average spectrum of three replicates of young lettuce leaves exposed to dark growth conditions, measured at 277 K, a) without addition of EDTA and b) with addition of EDTA during sample preparation. Arrows indicate signals undergoing significant changes.

In the high-field region (0-3 ppm), the use of EDTA triggers the release of some amino acids which makes a greater amount of signals in these region (Figure 3.8 b). As well, the citric, malic and succinic acid shows major differences in the NMR signals. These variations are difficult to explain and show that the EDTA interacts with the endogenous metabolites peaks, probably through the formation of complexes. In addition, the EDTA seems to chelate, not only with Ca^{2+}, but also with the Mg^{2+}. Since, in Figure 3.8 there is the appearance of characteristic signals at 2.56 and 2.76 ppm and in Figure 3.9 the signals at 3.09 and 3.23 ppm from Ca-EDTA^{2-} and Mg-EDTA^{2-}complexes respectively.

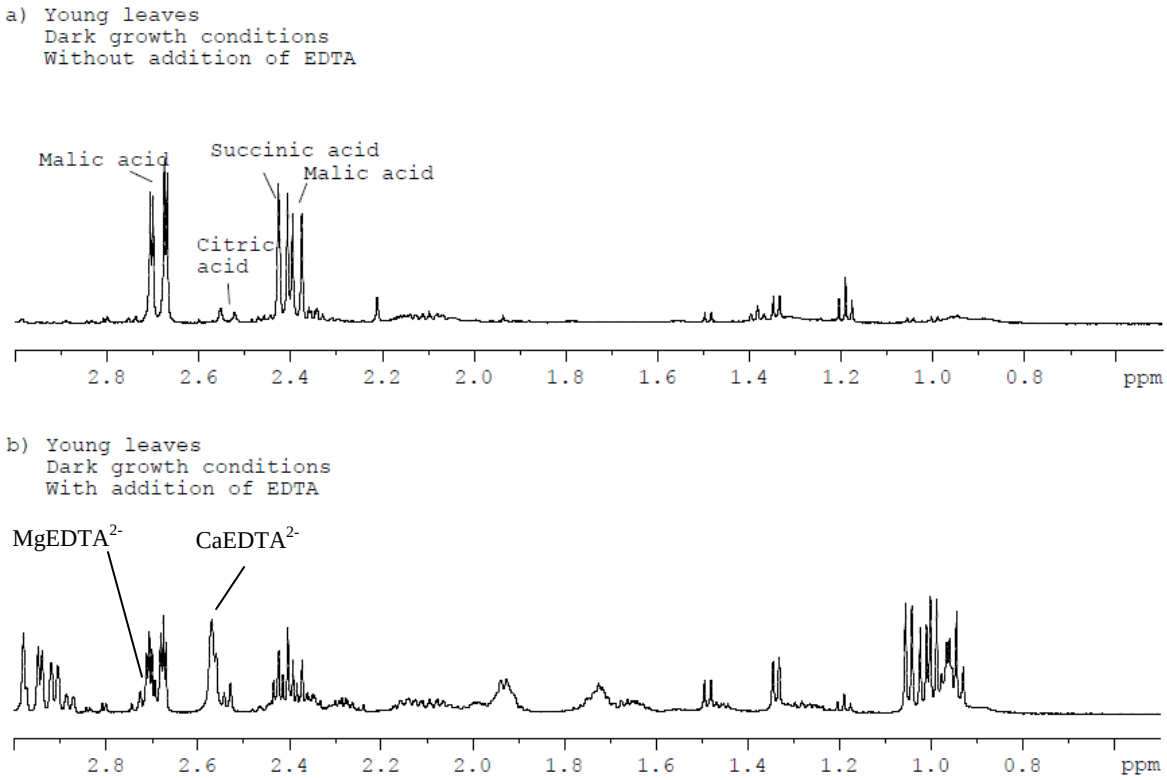

Figure 3.8: High-field region of the 500 MHz ^{1}H HRMAS NMR average spectrum of three replicates of young lettuce leaves exposed to dark growth conditions, measured at 277 K, a) without addition of EDTA and b) with addition of EDTA during sample preparation.

Regarding the mid field region, the addition of EDTA disables the identification of some signals, such as the peak belonging to the chemical shift at 4.66 and 5.26 ppm, which belongs to β-glucose and α-glucose, the signals of sucrose at 4.22 and 5.40 ppm and the signal of β-glucose at 3.25 ppm (indicated with arrows). Figure 3.9 b shows that some metabolite peaks are obscured by those from EDTA. Contrarily to the results presented by Barton et al. (2009), in which the NMR spectral effects of the EDTA with endogenous components from the plasma samples were insignificant.

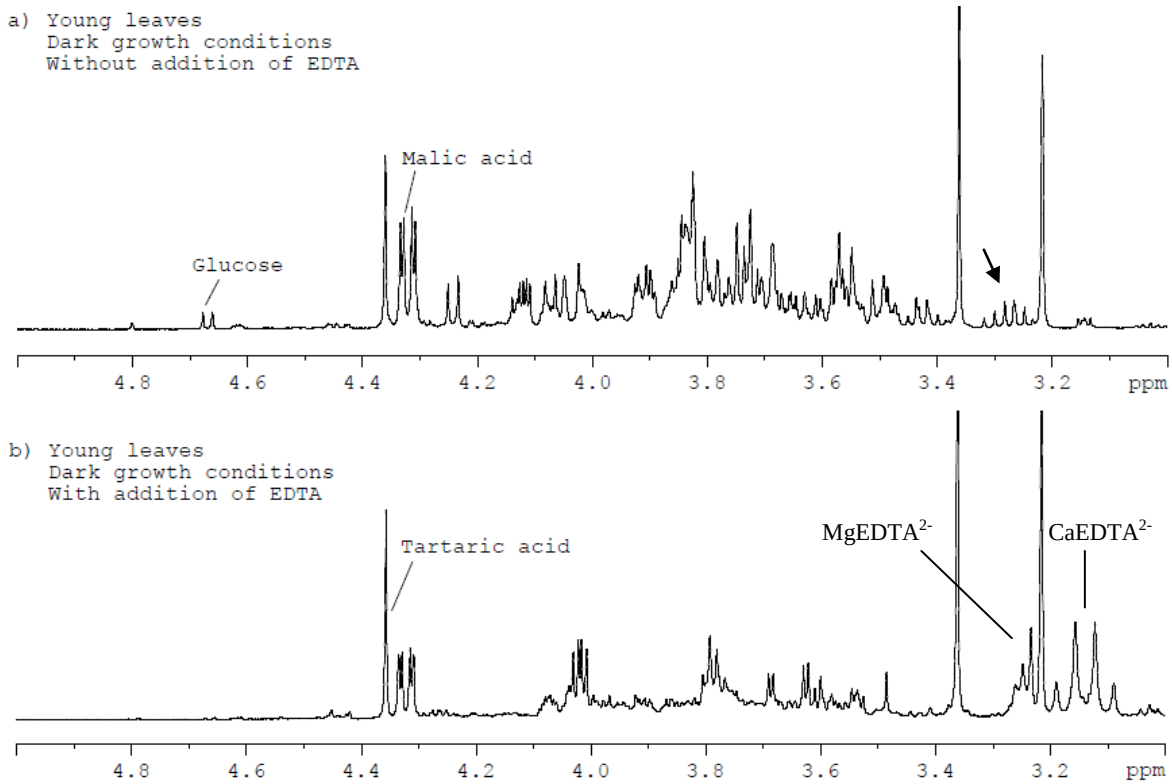

Figure 3.9: Mid-field region of the 500 MHz ^{1}H HRMAS NMR average spectrum of three replicates of young lettuce leaves exposed to dark growth conditions, measured at 277 K, a) without addition of EDTA and b) with addition of EDTA during sample preparation. Arrow indicates the β-glucose at 3.25 ppm.

In the low-field region (5.5-10 ppm), there are a greater number of NMR signals in the spectra of samples with EDTA added (Figure 3.10 b). Once more, it is difficult to explain these significant differences and these variations show that EDTA effect may depend on the region on the NMR spectra examined and the samples analyzed (Barton *et al.*, 2009)

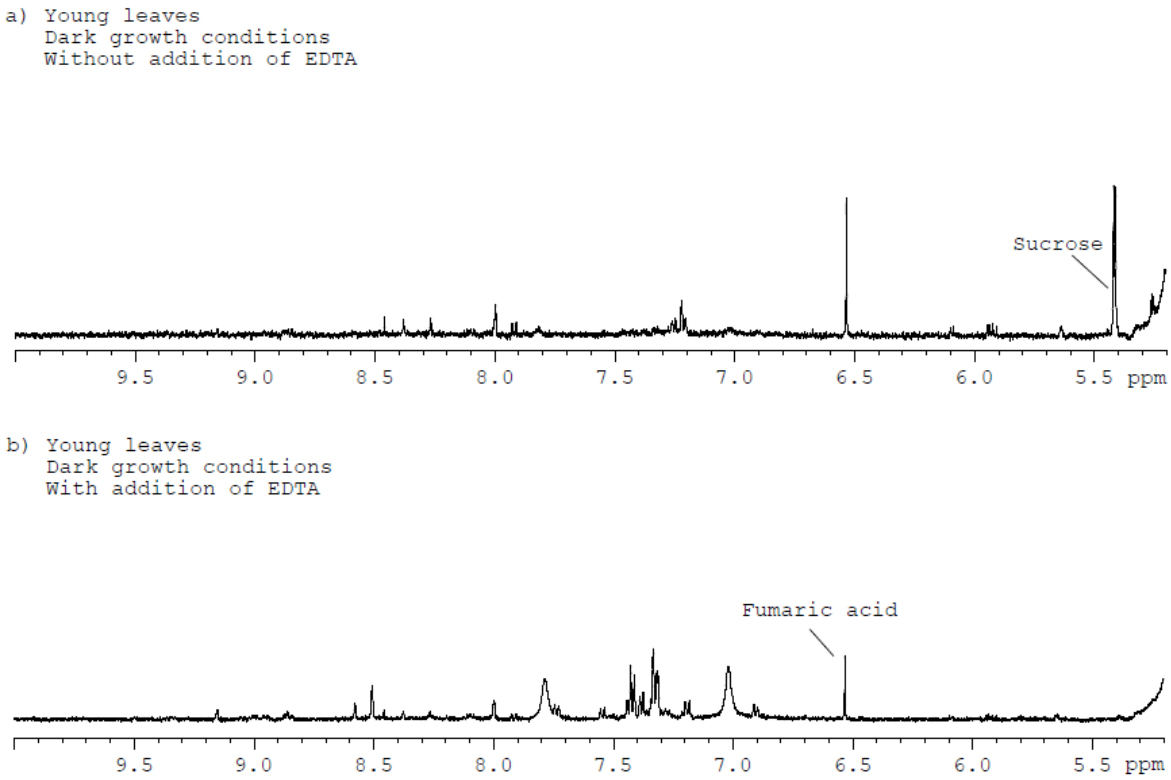

Figure 3.10: Low-field region of the 500 MHz ^{1}H HRMAS NMR average spectrum of three replicates of young lettuce leaves exposed to dark growth conditions, measured at 277 K, a) without addition of EDTA and b) with addition of EDTA during sample preparation.

3.2.2. Effects of the addition of EDTA to expanded and commercial lettuce leaves

In order to study the reproduction of EDTA results in the spectra of young lettuce leaves, the spectra of expanded leaves grown in dark and light conditions was also studied. In both conditions (light and dark), when the EDTA is used the expanded leaves spectra has greater resolution, since some metabolites have narrower signals (indicated with arrows). Furthermore, the EDTA binds the metal ion, Ca^{2+}, because in the Figure 3.11 b and d it appears the characteristic NMR signals resulting from formation of the Ca-EDTA^{2-} complex at 2.56 and 3.09 ppm.

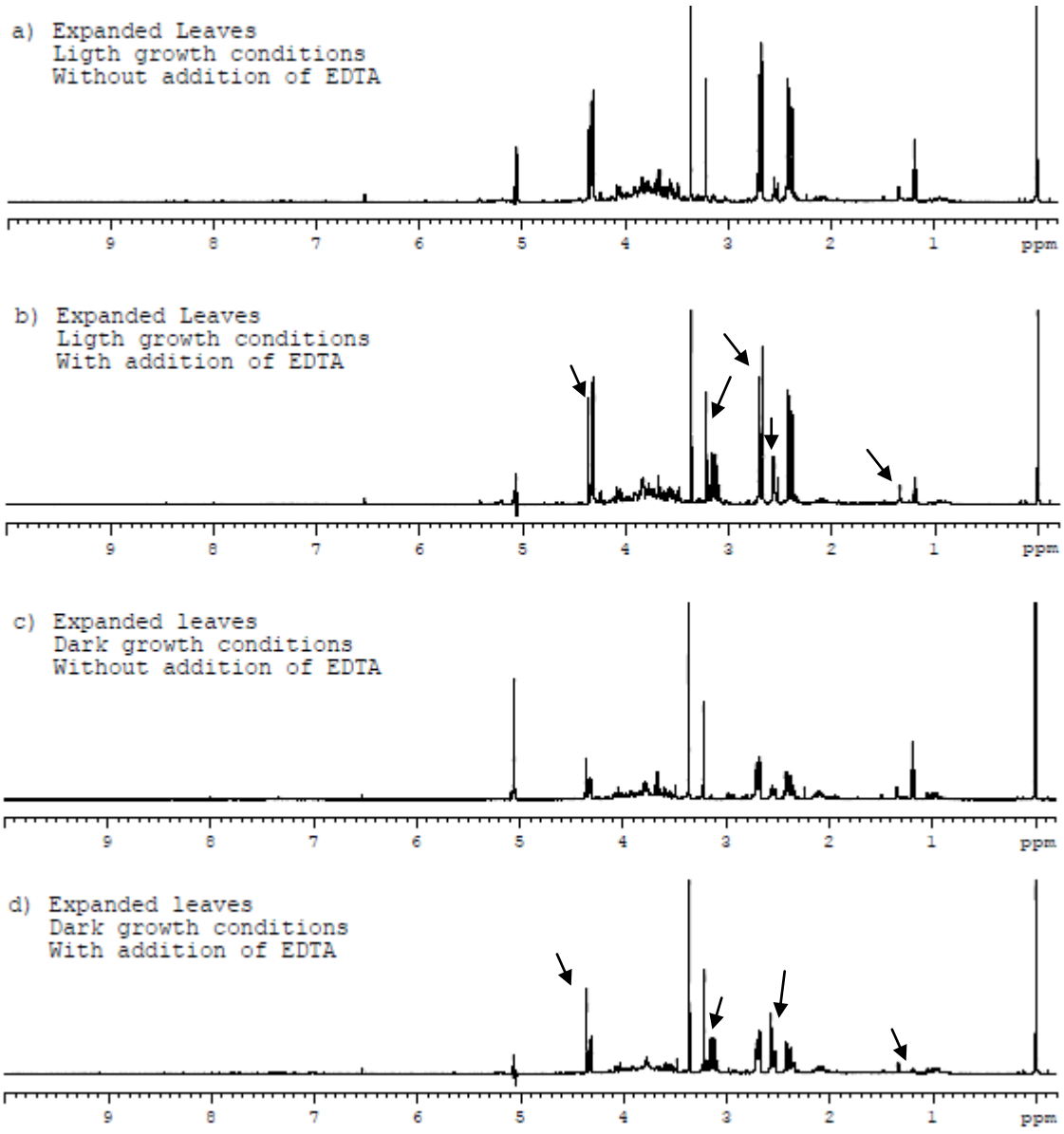

Figure 3.11: 500 MHz ^{1}H HRMAS NMR average spectrum of three replicates of expanded lettuce leaves exposed to light and dark growth conditions, measured at 277 K, a, c) without addition of EDTA, and b, d) with addition of EDTA during sample preparation respectively. Arrows indicate signals undergoing significant changes.

The last assay to study the effect of EDTA addition in the quality of the NMR spectra was performed in young leaves of commercial lettuce. Figure 3.12 b shows that the use of EDTA also results in an improvement of the resolution of the spectrum and that EDTA forms Ca-EDTA^{2-} complexes.

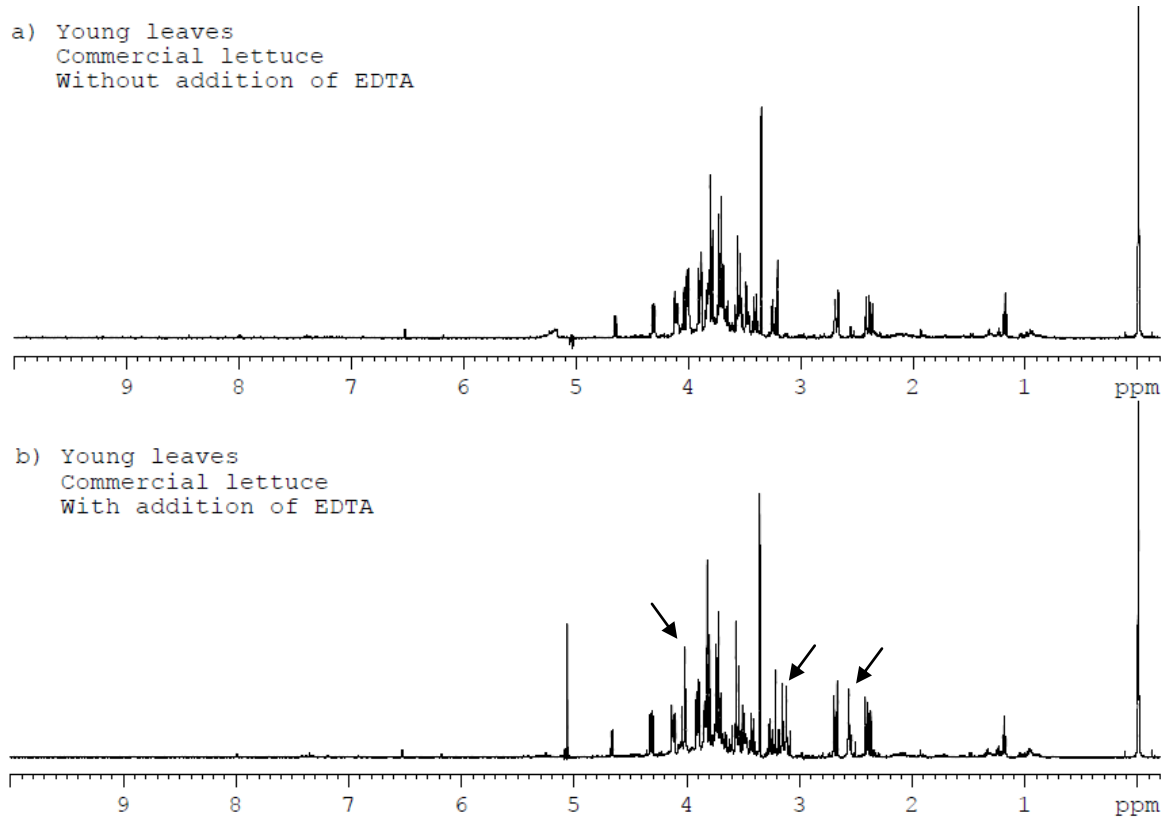

Figure 3.12: 500 MHz ^{1}H HRMAS NMR spectra of one replicate of young commercial lettuce leaves, measured at 277 K, a) without addition of EDTA and b) with addition of EDTA during sample preparation. Arrows indicate signals undergoing significant changes.

Although, the use of EDTA greatly affects the shape of ^{1}H NMR signals, which seems to enable a higher resolution on the signals of the spectra, the addition of signals from free EDTA and EDTA-metal complexes may cause a peak overlap with signals from endogenous compounds present in the lettuce. Moreover, the spectrum of young leaves in dark growth conditions with EDTA added shows that the use of EDTA allows a reduction in the line width of most of peaks, which implies a better resolution. Also in this spectrum, there is the addition of some NMR signals, which may make the interpretation more difficult. In the same way, it might complicate information retrieval for multivariate analysis. Therefore, in the following results presented in the thesis, it was chosen not to add EDTA during sample preparation.

3.3. Study of the Effects of Aging and Light Growth Conditions on the Metabolic and Physiological Response of Lettuce Leaves

This study tries to establish differences in the metabolism and physiology of lettuce leaves at different stages of maturity, i.e. young and expanded leaves metabolic changes was study by means of ^{1}H HRMAS NMR spectroscopy and the physiological variations by means of quantification of pigments content and chlorophyll *a* fluorescence measurements.

In the same way, the effect of different intensities during lettuce growth was assess, i.e. leaves were grown in light conditions (200 ± 20 µmol.m^{-2}.s^{-1}) and in dark conditions (20 ± 20 µmol.m^{-2}.s^{-1}).

3.3.1. Effects of aging and light growth conditions on the metabolic response of lettuce leaves

In Figure 3.13 the two top spectra are from young leaves and expanded leaves grown in light conditions and the two bottom spectra are from young leaves and expanded leaves grown in dark conditions.

Comparing the spectra of the young leaves with the spectra of expanded leaves in light growth conditions it is observable some differences in the metabolites present at different stages of growth. The main variations seem to occur in the mid-field region (3-5.5 ppm) in the carbohydrates profile. Variations in metabolism due to aging were expected since at the same conditions, the metabolome reflects the life history of each individual plant (Lindon *et al.*, 2007).

In the same way, when growing in dark conditions the young leaves and expanded leaves show some differences in some metabolites, due to a response to stress cause by a decrease on the intensity of the light (Figure 3.13).

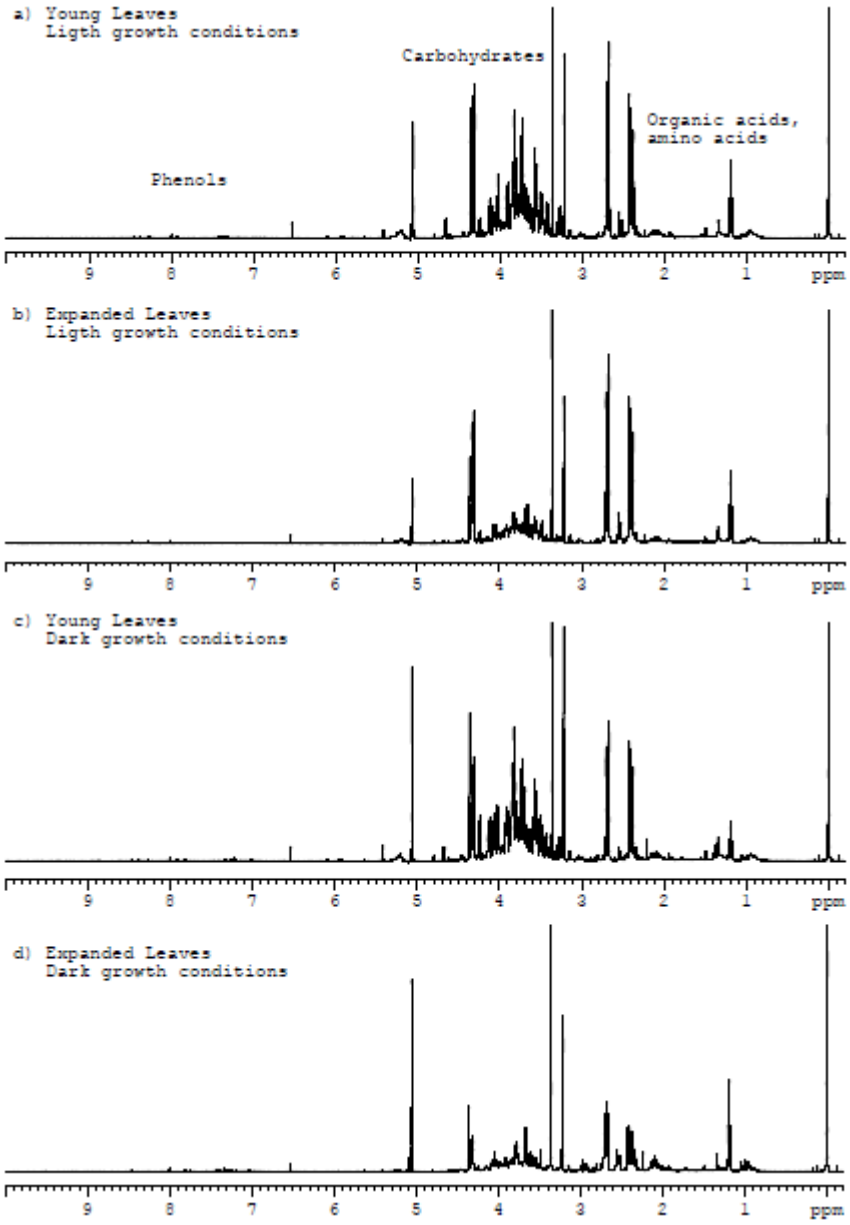

Figure 3.13: 500 MHz ^{1}H HRMAS NMR average spectrum of three replicates of a) young leaves and b) expanded leaves, lettuce plants exposed to light growth conditions, c) young lettuce leaves and d) expanded lettuce leaves, plants exposed to dark growth conditions, measured at 277 K.

The high-field region (0-3 ppm) of the spectra was horizontally expanded in the Figure 3.14, in order to facilitate the visualization of the variations that occur in this region. When comparing the leaves at different stages of growth, young (Figure 3.14 a) and expanded (Figure 3.14 b), the alanine peak at 1.47 shows a significant decrease relatively to the ethanol signal in the expanded leaves. Malic acid presents an increase relatively to

the ethanol signal in the expanded leaves. As well, the peak at 2.52 ppm arising from the citric acid increases relatively to the malic signal at 2.38 ppm in the expanded leaves.

In addition the Figure 3.14, the two bottom spectra, presents the variations that occur in leaves exposed to dark growth conditions. Both young and expanded leaves exposed to dark growth conditions (Figure 3.14 c and d) present significant differences in this region when compared to the light growth conditions (control) (Figure 3.14 a and b). As a response to the dark growth conditions the alanine peak, in both leaves, show a significant increase relatively to the lactic acid. The malic acid peaks decrease in both leaves exposed to dark growth conditions (Figure 3.14 b and d). Contrarily, the citric acid peak shows a decrease relatively to the malic signal at 2.38 ppm in the young leaves and shows a increase relatively to the same signal in the expanded leaves exposed to dark growth conditions (Figure 3.15). Furthermore, in stress the young leaves shows two unknown metabolites signal, at 1.37 and 2.21 ppm, with multiplicity of a triplet and singlet respectively (indicated with arrows in Figure 3.14 c).

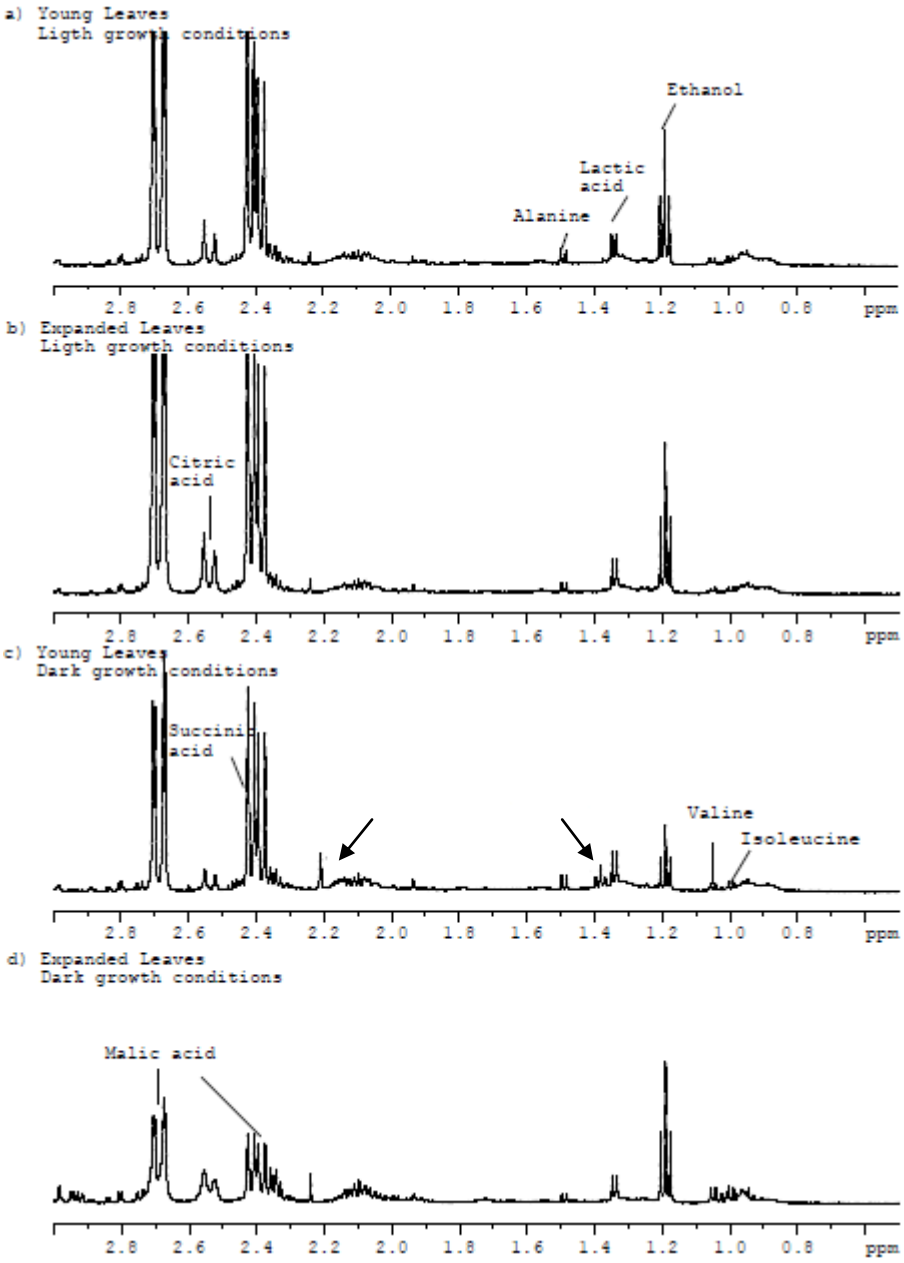

Figure 3.14: High-field region of the 500 MHz ^{1}H HRMAS NMR average spectrum of three replicates of a) young leaves and b) expanded leaves, lettuce plants exposed to light growth conditions, c) young lettuce leaves and d) expanded lettuce leaves, plants exposed to dark growth conditions, measured at 277 K. Peaks indicated with arrows show unassigned compounds with significant variation.

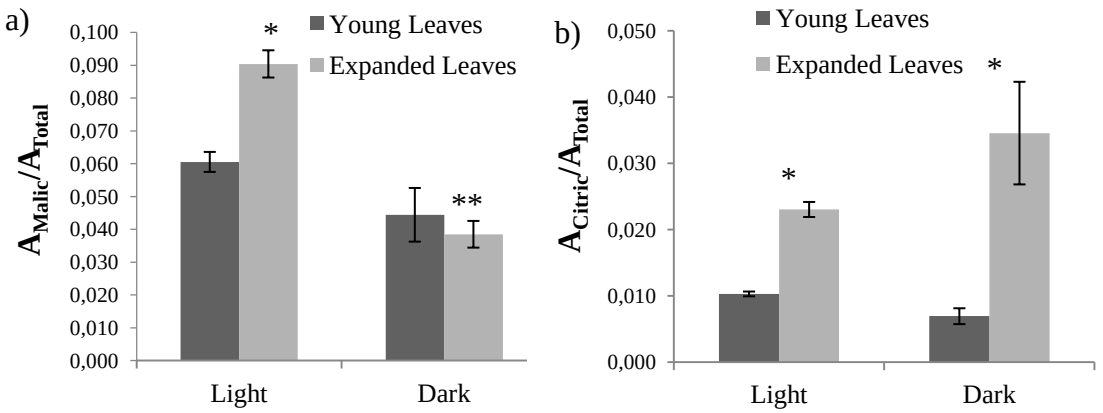

Figure 3.15: Plots of area ratios (to total spectral area) for a) malic and b) citric acids during ageing and light/dark growth conditions. (*) significant differences and (**) no significant differences between aging of leaves, both in same conditions, at a significant level lower than 0.05.

In the mid-field region (3 to 5.5 ppm), are present some differences that occur because of the aging of the leaves and because of the conditions on growth. Concerning the sugars content, when comparing young to expanded leaves, the β-glucose peaks at 3.40 and 4.66 ppm show a decrease relatively to the sucrose signal at 4.22 ppm in the expanded leaves. As well, the fructose peak at 4.12 ppm presents a decrease relatively to the sucrose signal in the expanded leaves. The sucrose peaks at 4.22 and 5.40 ppm also show a significant decrease in the expanded leaves relatively to the tartaric acid signal at 4.34 ppm. Moreover, the peak at 4.34 ppm arising from the tartaric acid decrease in the expanded leaves (Figure 3.16 b). Contrarily to our results, the work performed by Shuib et *al.*, (2010), using ^{1}H NMR spectroscopy and multivariate data analysis that the expanded leaves of *Melicope ptelefolia* tree contain higher levels of sugars. This could be explain because only the excess of organic compounds resulting from the photosynthesis, in particular the sugars, produced in mature leaves are exported to young leaves (Choi *et al.*, 2004). However, the discordance of results may be due to the difference on the time of growth of the tree and lettuce plant. In addition, sugars provide the secondary metabolites needed for the synthesis of macromolecules and other cell constituents (Rosa *et al.*, 2009), which suggests that the sugars in expanded leaves are been mobilized for example for synthesis of cell wall constituents.

In response to the stress caused by dark growth conditions, the β-glucose peaks at 3.40 and 4.66 ppm decrease relatively to the tartaric acid signal in both leaves. The sucrose peaks 4.22 and 5.40 ppm (illustrated in Figure 3.16) ppm increase relatively to the glucose signal in the young leaves (Figure 3.16 c) and decrease relatively to malic acid signal at 4.30 ppm in the expanded leaves (Figure 3.16 d). The glucose and sucrose sugars were quantified by integrating the β-glucose doublet signal at 4.66 ppm and the sucrose doublet signal at 5.40 ppm. The quantification results are shown in Figure 3.17.

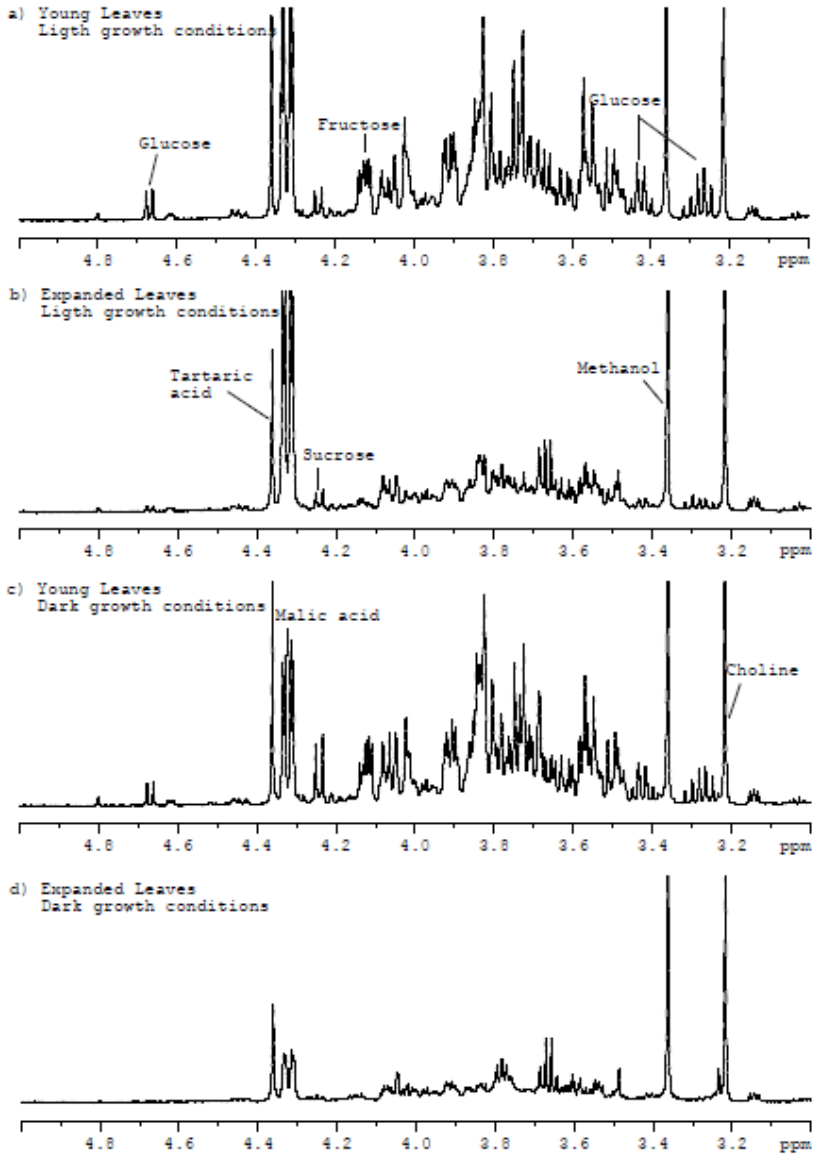

Figure 3.16: Mid-field region of the 500 MHz ^{1}H HRMAS NMR average spectrum of three replicates of a) young leaves and b) expanded leaves, lettuce plants exposed to light growth conditions, c) young lettuce leaves and d) expanded lettuce leaves, plants exposed to dark growth conditions, measured at 277 K.

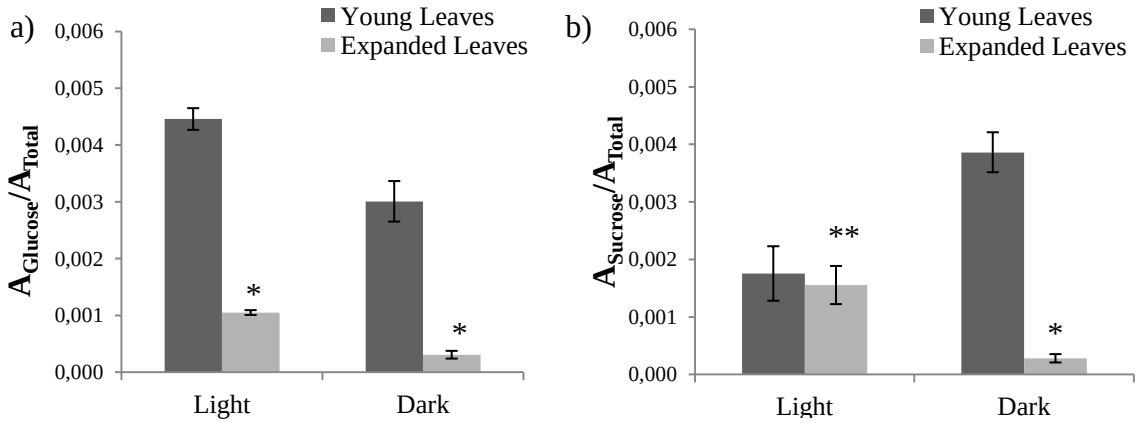

Figure 3.17: Plots of area ratios (to total spectral area) for a) glucose and b) sucrose sugars during ageing and light/dark growth conditions. (*) significant differences and (**) no significant differences between aging of leaves, both in same conditions, at a significant level lower than 0.05.

These results suggest that due to variations in light intensity there is a decrease in the photosynthesis (discussed in section 3.3.2) which lead to a reduce supply of sugars in expanded leaves (Rosa *et al.*, 2009). A similar study on the influence of light regimes on carbohydrates content in mature leaves of *Ajuga Reptains* L. was performed by Pystina and Danilov (2001) show that the carbohydatres decreased signiflicantly in the mature leaves of shade plants (grown in an reduced light environment).

In the low-field region, the major difference seems to be in fumaric acid peak at 6.54 ppm which decreases relatively to sucrose signal at 5.40 ppm in the expanded leaves (illustrated in the two top spectra in Figure 3.18). Moreover, both young and expanded leaves present unassigned signals from 8.0-8.5 ppm which suggests the presence of phenolic compounds in both leaves.

In dark growth conditions, both leaves present unassigned systems from 7.00 to 7.44, suggestion the presence of phenylalanine and tyrosine and from 8.0 to 7.90 ppm (illustrated with arrows in Figure 3.18 c and d) which suggest the presence of phenolic compounds. The presence of these metabolites may be a result of plant protective mechanism against the stress caused by dark growth conditions, since the phenylalanine and tyrosine are known to be precursors for a wide variety of phenolic compounds (Oh *et al.*, 2009a; Wang *et al.*, 2011).

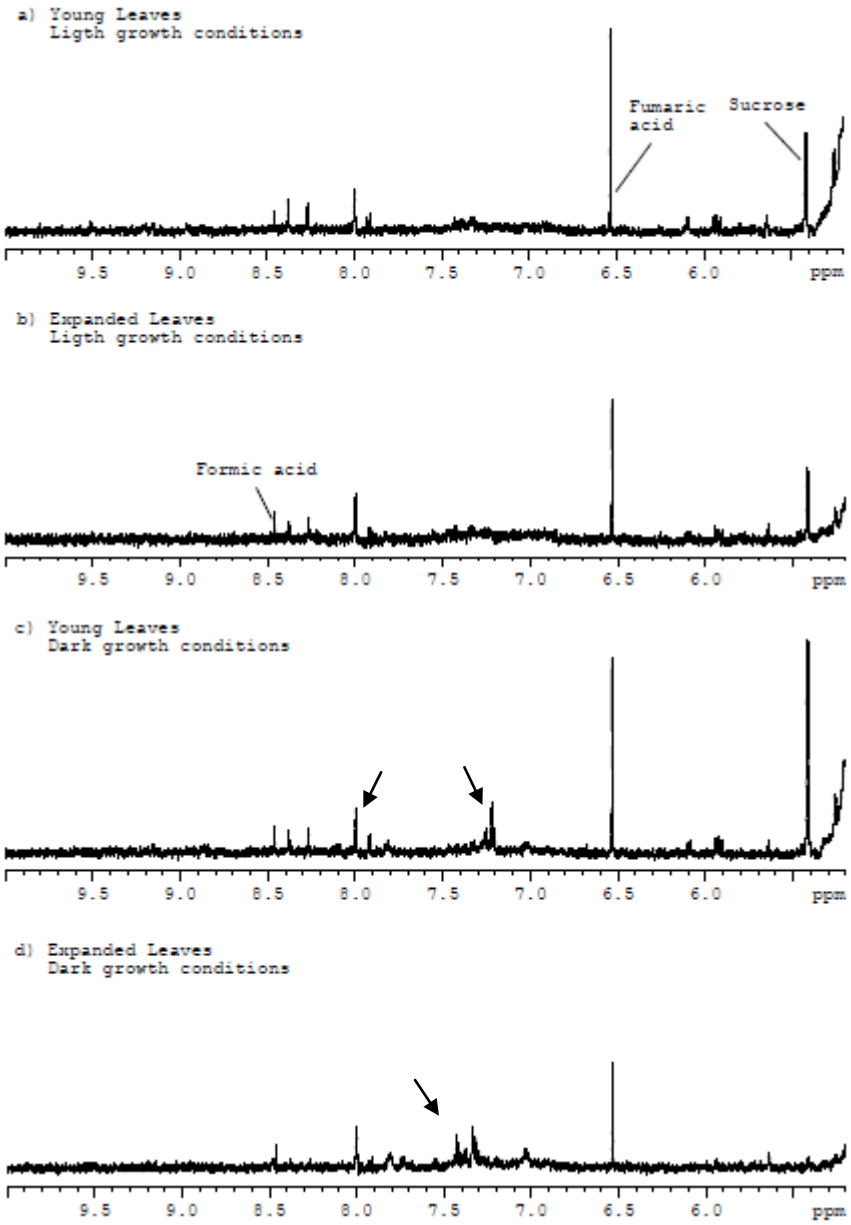

Figure 3.18: Low-field region of the 500 MHz ^{1}H HRMAS NMR average spectrum of three replicates of a) young leaves and b) expanded leaves, lettuce plants exposed to light growth conditions, c) young lettuce leaves and d) expanded lettuce leaves, plants exposed to dark growth conditions, measured at 277 K. Peaks indicated with arrows show unassigned compounds with significant variation.

3.3.2. Effects of aging and light growth conditions on the physiological response of lettuce leaves

In order to study the physiological differences in young and expanded lettuce leaves exposed to light and dark growth conditions, chlorophyll content and photosynthetic efficiency were determined after 7 days of exposure to these growth conditions (Table 3.2).

No visible changes in growth or leaf morphology between dark and light exposed lettuce plants were observed. Moreover, no necrosis symptoms and leaf fall were visible in dark exposed lettuce plants. This is indicates that the lettuce leaves did not present any symptom of stress due to aging and light growth conditions (Monteiro *et al.*, 2009).

Table 3.2: Effects of aging and light growth conditions on chlorophyll content and on fluorescence parameters in young and expanded leaves of lettuce. Values are means ± standard deviation (SD) (n=6); (*) significantly different from leaves grown in light conditions.

Photosynthetic parameters	**Young leaves**		**Expanded leaves**	
	Light	Dark	Light	Dark
Chlorophyll content *(µmol/g FW)*				
Chl *a*	0.60 ± 0.1	0.45 ± 0.08*	0.59 ± 0.15	0.35 ± 0.05*
Chl *b*	0.14 ± 0.08	0.13 ± 0.08	0.22 ± 0.07	0.13 ± 0.04
Carotenoids	0.34 ± 0.02	0.31 ± 0.04	0.38 ± 0.1	0.30 ± 0.02
Fluorescence parameters				
F_v/F_m	0.80 ± 0.04	0.82 ± 0.03	0.83 ± 0.02	0.81± 0.02*
Φ_{PSII}	0.78 ± 0.001	0.72 ± 0.09*	0.78 ±0.03	0.64 ± 0.04*

As it can be seen in table 3.2, between young and expanded leaves there were no significant changes in the pigments content and in the fluorescence measurements. In older leaves generally is expected a decrease in the photosynthetic efficiency (Whitehead *et al.*, 2010).

Contrarily, the lettuce plants grown in dark conditions exhibit a significant lower content of Chl *a* than leaves exposed to light growth conditions. On the other hand, this leaves do not display a significant difference considering Chl *b* and carotenoids content. However, when plants are under stress the Chl tends to decline more rapidly than carotenoids content (Sims and Gamon, 2002). The work of Lichtenthaler *et al.* (2007) show that the chl *a* and *b* and carotenoids content levels between sun and shade lights decrease in leaves of four tree species that grown in shade.

Considering the Chl *a* fluorescence parameters, no significant differences were observed in the photosynthetic efficiency (F_v/F_m) of light and dark exposed young leaves. As a result, the young leaves do not present a reduction of the photosynthetic performance due to differences of light during growth. Contrarily, in expanded leaves the F_v/F_m decreased significantly under dark condition compared to control leaves, but, the values obtained are typical for healthy plants (Schreiber *et al.*, 1995). Thus, dark growth conditions reduced the photosynthetic performance of expanded leaves. Another parameters measured was the quantum efficiency of PSII (Φ_{PSII}). Φ_{PSII} in dark exposed young and expanded leaves presented a significant decrease in comparison to leaves grown in light conditions. Thus, the decrease in the proportion of the light absorbed by chlorophyll associated with PSII that is used in photochemistry (Φ_{PSII}) under dark conditions may be attributed to the significant reduction of the Chl *a* observed in these leaves and suggest some photoinhibition (Martin *et al.*, 2010). Similarly to our results, the study on the photosynthetic responses in Norway spruce shown that the sun leaves had higher rates of photosynthesis (Bertamini *et al.*, 2006).

3.4. Study of the Effects of Mancozeb Exposure on the Metabolic and Physiological Response of Lettuce Leaves

In order to study the effects caused by the mancozeb in the lettuce metabolome and physiology, young and expanded lettuce leaves were exposed to this pesticide, in light growth conditions, and 7 days after exposure analyzed through ^{1}H HRMAS NMR spectroscopy. In the same conditions but without exposure to the mancozeb, young and expanded leaves (control plants) were also analyzed. Following exposure of mancozeb in lettuce leaves, the effects of the mancozeb might be recognizable in the plant's metabolic

response and in the physiological performance (discussed on the next subchapter), in a way that will be possible to pinpoint putative metabolic and photosynthetic biomarkers.

3.4.1. Effects of mancozeb on the metabolic response of lettuce leaves

In Figure 3.19 it is clearly noticeable some variations in the metabolic profile on the leaves exposed to mancozeb comparing with the spectra of controls. Both young and expanded leaves spectra show differences from the controls, in the region of organic acids and amino acids (high-field region) and on the region of carbohydrates (mid-field region). For a better understanding of the variations of metabolites known to be present on lettuce leaves, the high-field region (0-3 ppm), and mid-field region (3-5.5 ppm) were horizontally expanded in Figure 3.20 and Figure 3.23 respectively.

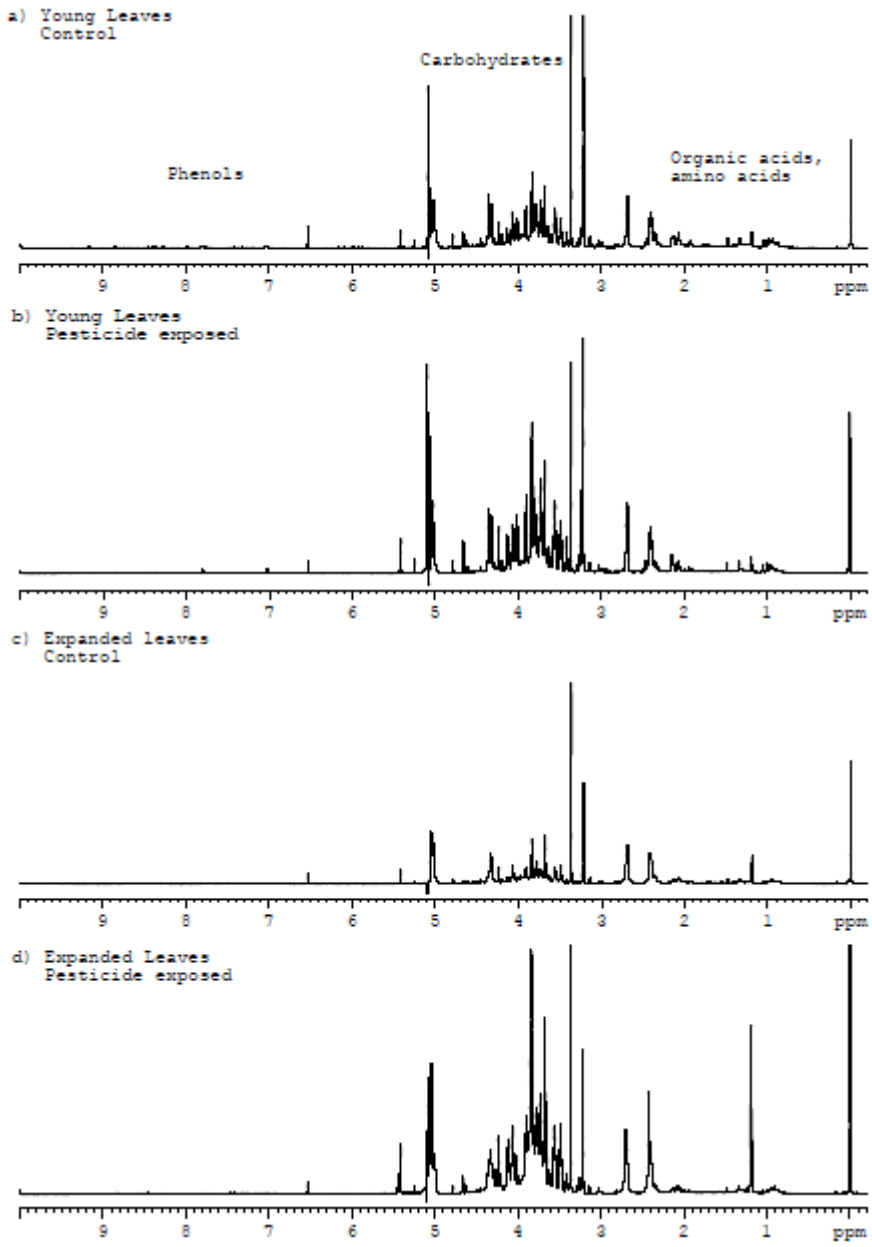

Figure 3.19: 800 MHz ^{1}H HRMAS NMR spectra of lettuce leaves average spectrum of four replicates of a), c) young and expanded (control), b) and d) young and expanded exposed to mancozeb, measured at 277 K.

In the high-field region (Figure 3.20), some variations are noticed in terms of some organic acids and amino acids profile. Malic and lactic acid are presented both in young and expanded leaves, and show smaller variations in young leaves exposed to mancozeb (illustrated in Figure 3.20 by the two top spectra) because in the expanded leaves exposed to mancozeb there is a significant decrease of lactic acid and malic acid (illustrated in

Figure 3.20 by the two bottom spectra). The lactic and malic acids were quantified through integration of the signals at 1.32 and 2.67 ppm and are present in Figure 3.21. The lower resolution of the malic acid signal at 2.38 and 2.67 ppm, suggests the interaction with other components, for example by means of the formation of complexes. Concerning the amino acids, valine, and alanine are seen to decrease in both leaves exposed to mancozeb, as shown by the quantitative results presented in the Figure 3.22.

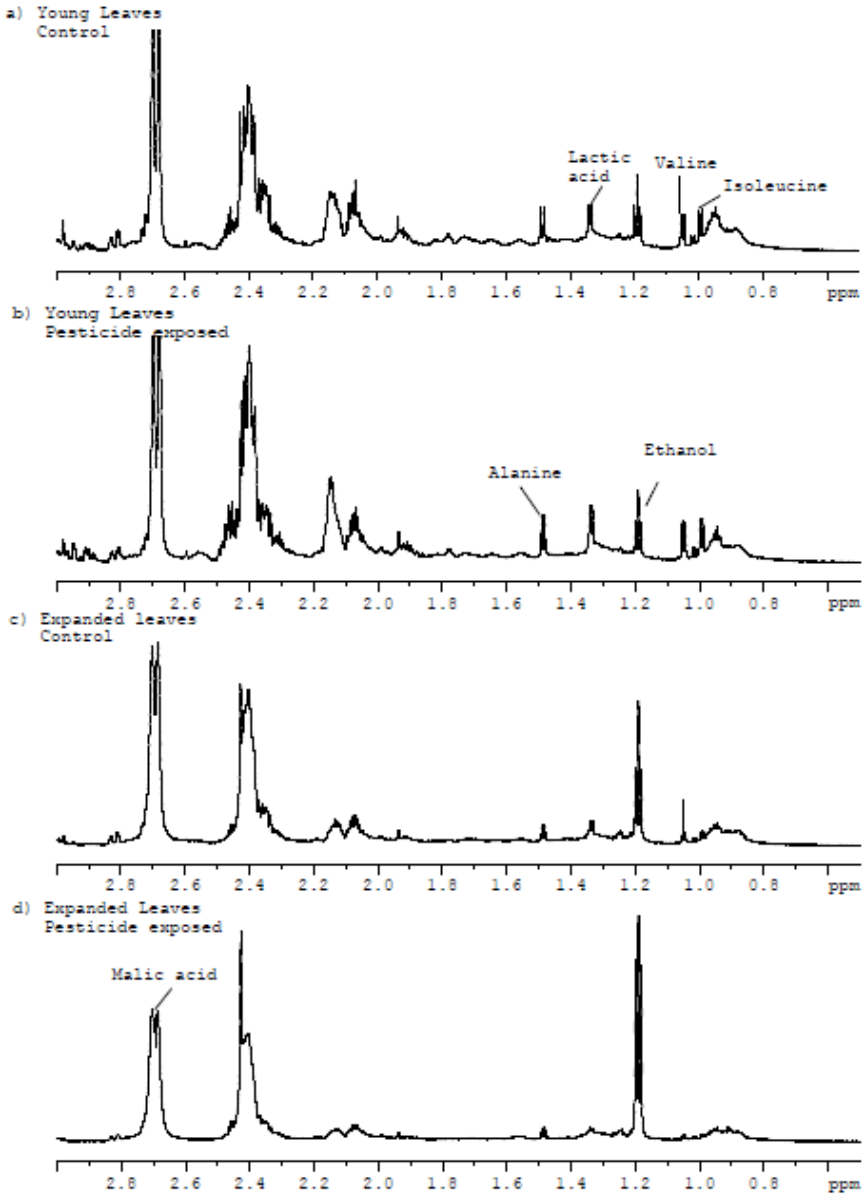

Figure 3.20: High-field region of the 800 MHz ^{1}H HRMAS NMR spectra of lettuce leaves average spectrum of four replicates of a), c) young and expanded (control), b) and d) young and expanded exposed to mancozeb, measured at 277 K.

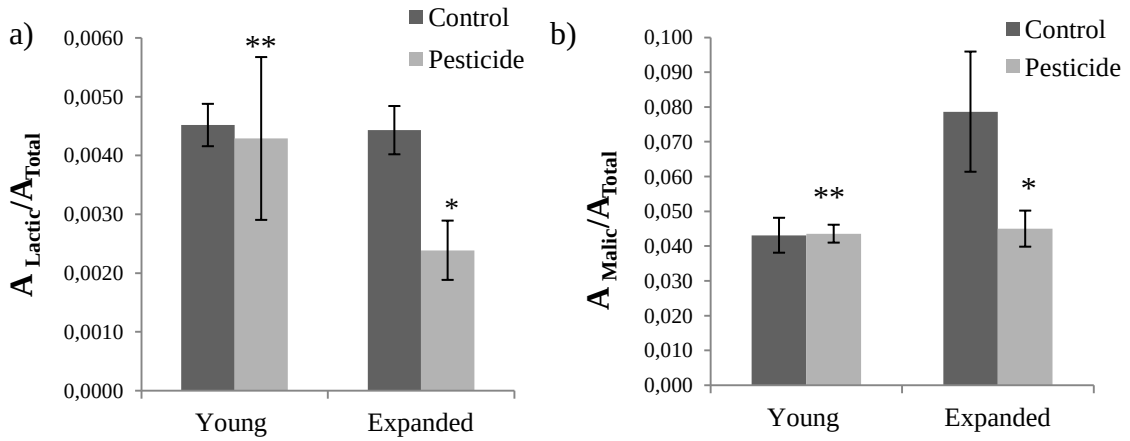

Figure 3.21: Plots of area ratios (to total spectral area) for a) lactic and b) malic acid sugars during exposure to mancozeb. (*) significant differences and (**) no significant differences between conditions, at a significant level lower than 0.05.

The amino acids quantified were, valine and alanine. For valine the signal at 1.04 ppm was integrated. The alanine was quantified by the doublet signal at 1.48 ppm. The results presented show that the content of valine and alanine is lower in leaves exposed to mancozeb (Figure 3.22). The amino acids are primary metabolites of plants which are involved in plant growth, reproduction and energy generation and the mancozeb exposure seems to inhibit the synthesis of amino acids in leaves (Ali *et al.*, 2009).

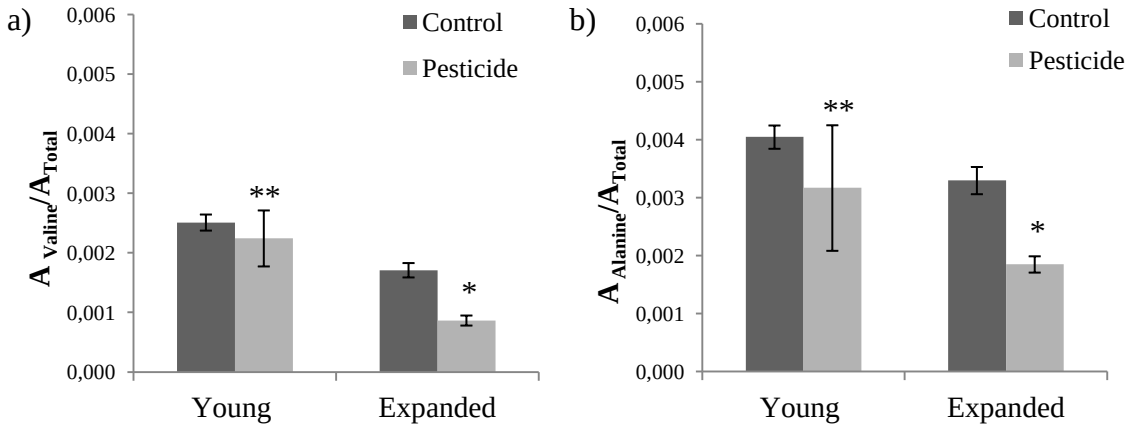

Figure 3.22: Plots of area ratios (to total spectral area) for a) valine and b) alanine amino acids during exposure to mancozeb. (*) significant differences and (**) no significant differences between conditions, at a significant level lower than 0.05.

The variations on the spectra in the sugar region are shown in Figure 3.23. Concerning the major sugars (glucose, fructose and sucrose), it is noticeable that the exposure to mancozeb, in young and expanded leaves, induced an increase in the proportions of these sugars. By comparing the relative intensities of non-overlapped signals it is possible to assess these differences. The sucrose peaks at 4.22 and 5.40 ppm demonstrate an increase relatively to glucose and fructose signals. The β-glucose peaks at 3.41 (indicated with arrows in Figure 3.23) and 4.66 ppm and the α-glucose peak at 5.26 ppm (illustrated in Figure 3.23) show an increase during exposure to mancozeb but comparatively to sucrose are still lower in the leaves of lettuce. As well the sucrose peak at 4.22 and 5.40 ppm (illustrated in Figure 3.25) clearly increases during exposure to mancozeb. With the quantification results obtained for these sugars it is easy to understand the variations on the intensity, which are presented in Figure 3.24.

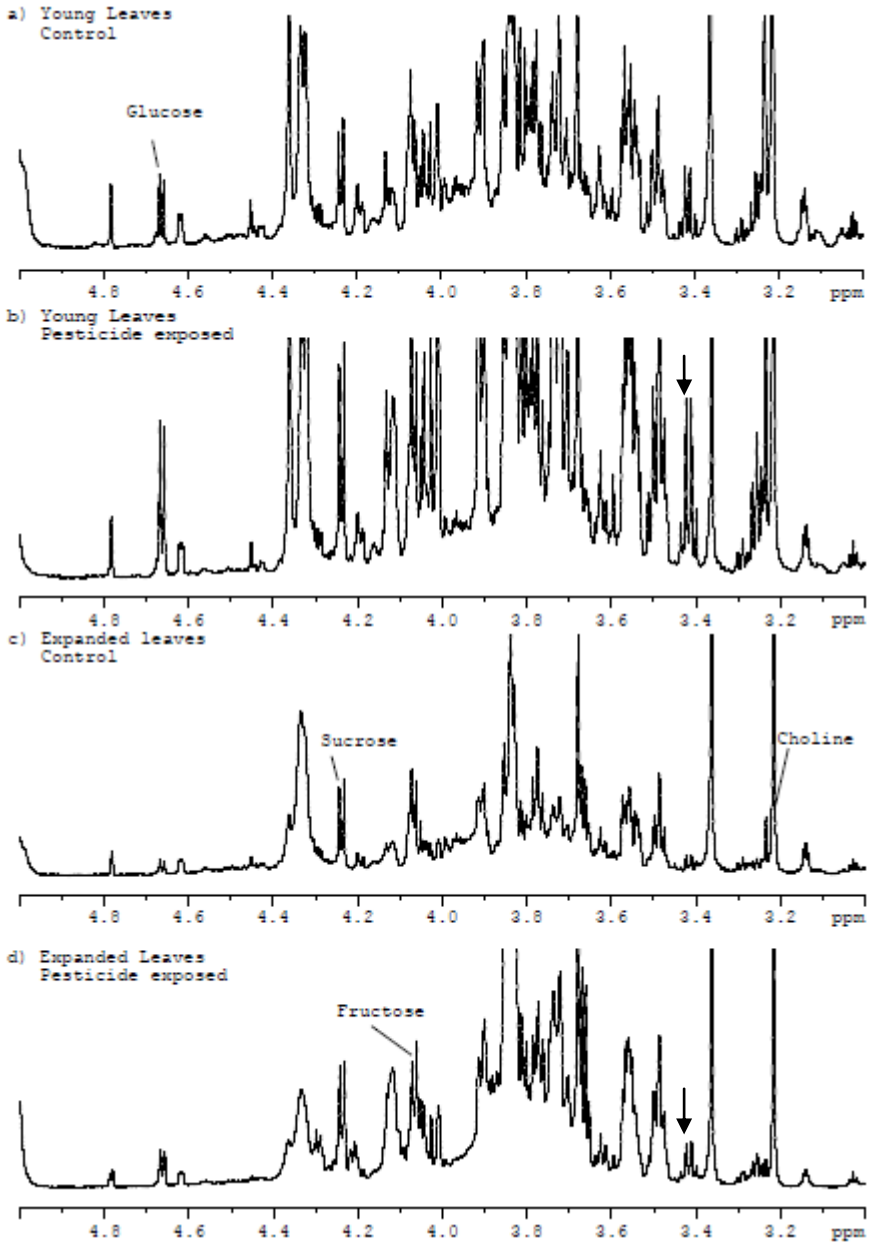

Figure 3.23: Mid-field region of the 800 MHz ^{1}H HRMAS NMR spectra of lettuce leaves average spectrum of four replicates of a), c) young and expanded (control), b) and d) young and expanded exposed to mancozeb, measured at 277 K.

Figure 3.24 shows the quantification by integrating the signals of α-glucose at 5.26 ppm and sucrose at 5.40 ppm. Mancozeb induced an accumulation of sucrose and glucose on lettuce leaves. These results are in agreement with those observed in the work of Saladin *et al.* (2003) in which the treatment of *Vitis vinifera* L.with flumiozaxin (herbicide) resulted in an accumulation of sugars (glucose, fructose and sucrose) in every organ of the

plantlets. The accumulation of sugar in lettuce leaves exposed to mancozeb indicates a inhibition of the photosynthesis (discussed in section 3.4.2) and may be due to an inhibition of the short distance transport of the biological compounds formed by assimilation using light-dependent reactions. In addition, the increase of sucrose in leaves treated with mancozeb suggests a reduction of carbohydrates transport to the leaves. (Saladin *et al.*, 2003a) and a reduction in growth.

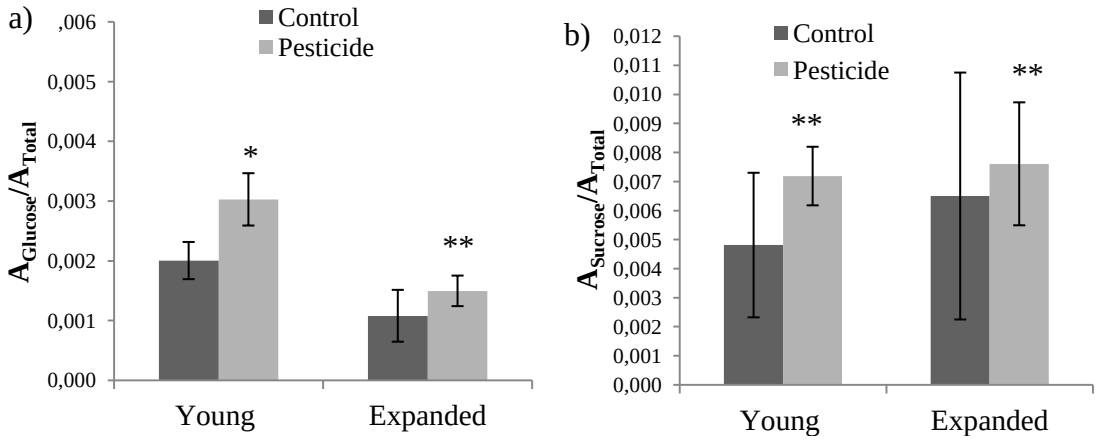

Figure 3.24: Plots of area ratios (to total spectral area) for a) glucose and b) sucrose sugars during exposure to mancozeb. (*) significant differences and (**) no significant differences between conditions, at a significant level lower than 0.05.

Figure 3.25 illustrates the alterations in the low-field region on the lettuce spectra when exposed to mancozeb. In this region only the signals of glucose, sucrose, fumaric and formic acid, were successfully identified. Nevertheless, some differences occur in this region. The fumaric acid relatively to the sucrose signal at 5.40 ppm shows a decrease in the leaves exposed to mancozeb. The unassigned signals at 7.02 and 7.80 ppm only appear in young leaves, and are increased in the young leaves exposed to mancozeb (indicated with arrows in Figure 3.26). These results suggest the synthesis of phenolic compounds in leaves exposed to mancozeb (Ali *et al.*, 2009). Other spectral changes in this region regard another unassigned signal at 5.43 ppm (indicated with arrows in Figure 3.25), which increases during exposure to mancozeb in young and in expanded leaves.

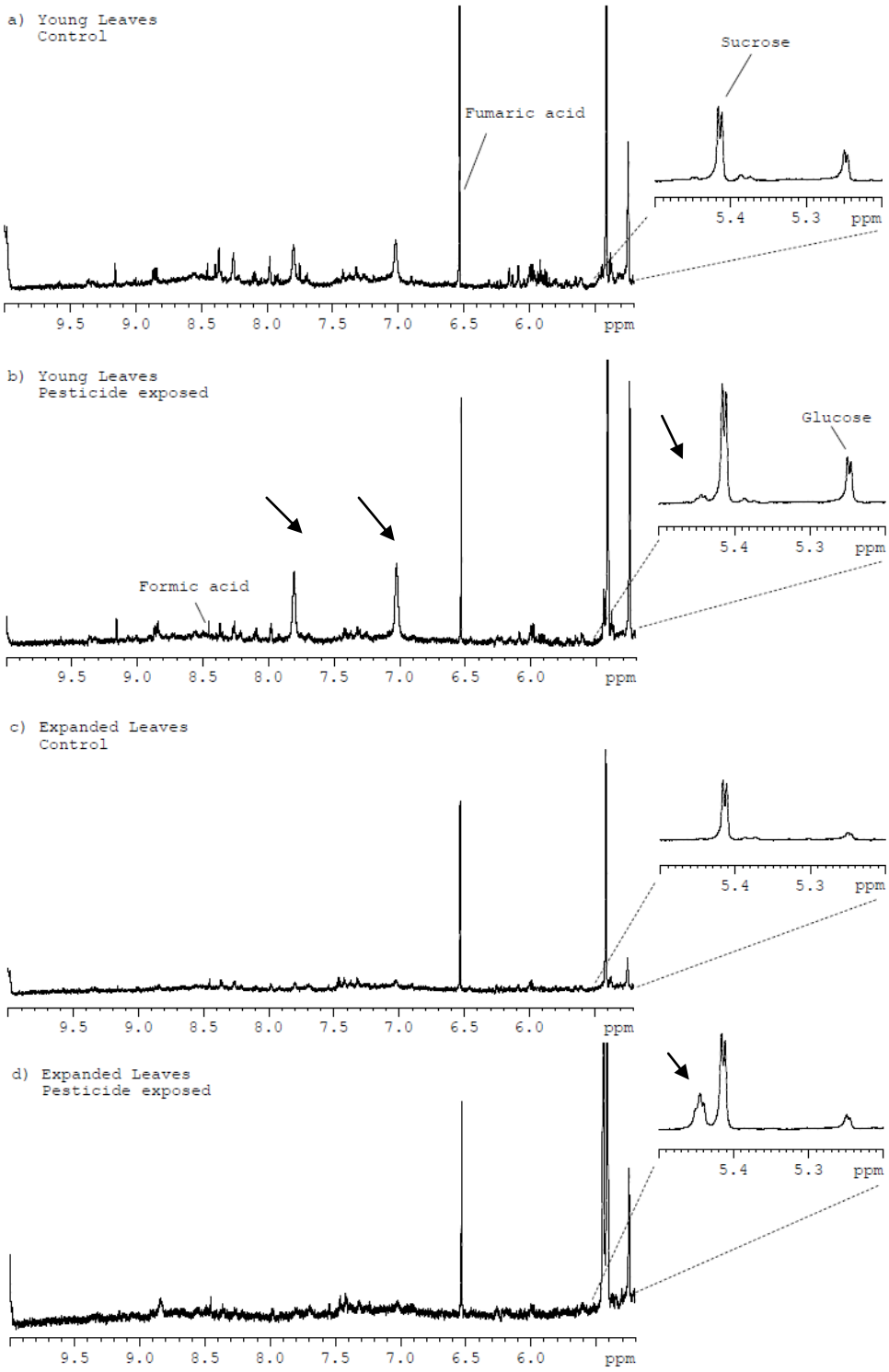

Figure 3.25: Low-field region of the of the 800 MHz ^{1}H HRMAS NMR spectra of lettuce leaves average spectrum of four replicates of a), c) young and expanded (control), b) and d) young and expanded exposed to mancozeb, measured at 277 K. The insets show expansions of the low-field region (5.2-5.5 ppm)

3.4.2. Effects of mancozeb on the physiological response of lettuce leaves

It is known that photosynthesis can be inhibited at several levels, such as photosynthetic pigments synthesis, electron transport, enzymes of the Calvin cycle and uptake of nutrients. Numerous studies, for example, on growth rate, Chl *a* fluorescence were used to elucidate the mode of action of herbicides on plant (Xia *et al.,* 2006). In order to understand the changes that occur in the photosynthetic apparatus of lettuce treated with mancozeb, the variations on the photosynthetic pigments and on the plant photochemical processes were measured.

Change on the morphology of the leaves, in particular chlorosis, is one of the most common signals of damage on the photosynthetic pigments biosynthesis pathways (Baryla *et al.,* 2001). In the same way, as observed in plants exposed to light/dark growth conditions, no morphological change was noticed in the plants exposed to mancozeb. These observations are not consistent with the measurements on pigment contents (Figure 3.26) and Chl a fluorescence parameters (Figure 3.27), which are reliable indicators of photosynthetic apparatus state, because there are some significant physiological differences.

In what concerns the pigments content measurements the young leaves exposed to mancozeb contained lower contents of Chl *a*, Chl *b* and carotenoids than control leaves ($P<0.05$) (Figure 3.26 B, D and F). However, in expanded leaves exposed to mancozeb only the concentration of Chl *a* was negatively affected ($P<0.05$). No significant differences were observed in Chl *b* and carotenoids on these leaves (Figure 3.26 A, C and E).

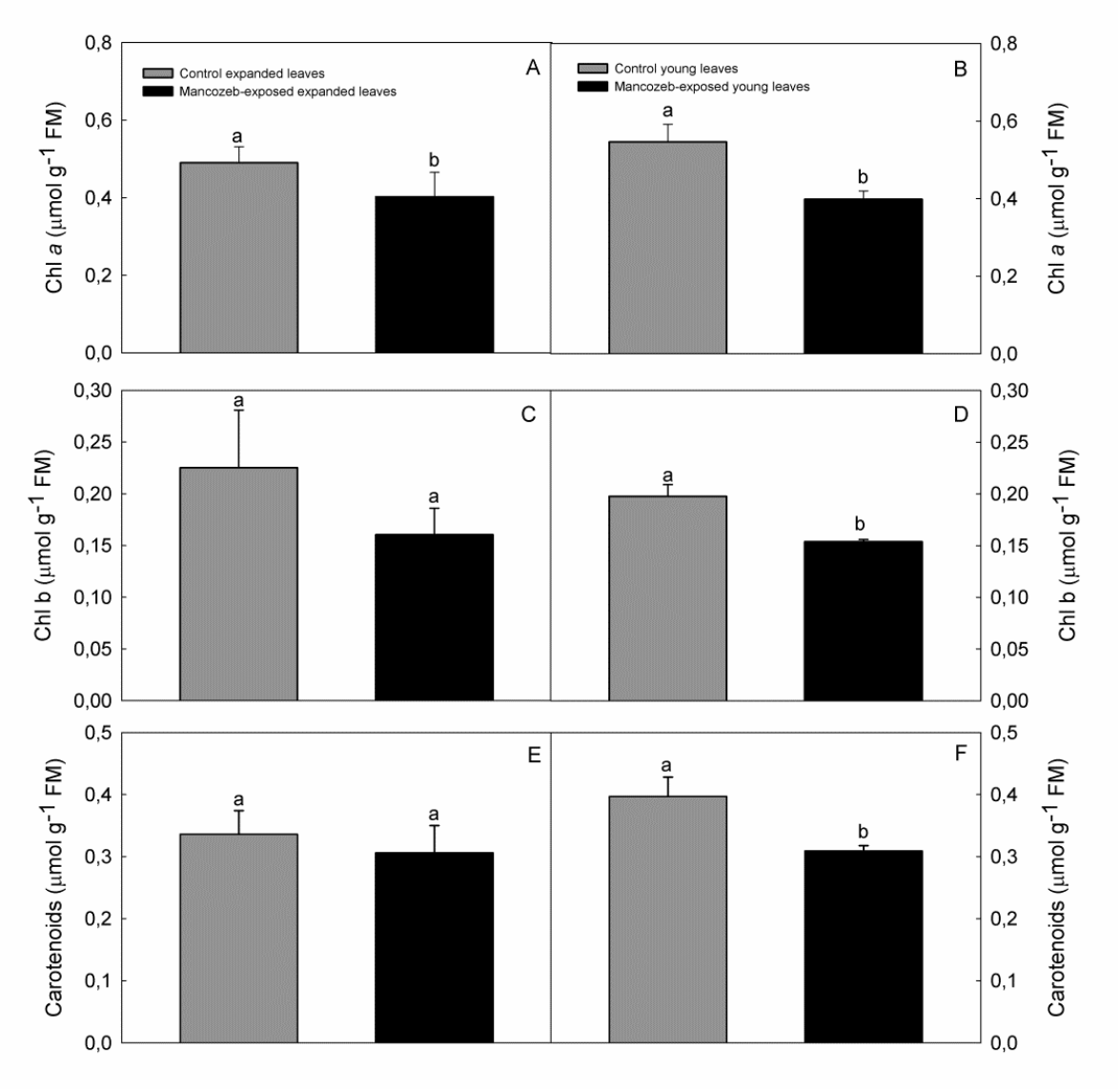

Figure 3.26: Effect of mancozeb stress on Chl *a*, chl *b* and carotenoids content in expanded and young leaves of lettuce after 7 days of exposure. Values are means ± SD (n=6). Different letters indicate significant differences between treatments at a significant level equal to 0.05.

These results demonstrated that in young leaves the stress caused by the mancozeb was more severe because the pigment biosynthesis seems to be suppressed. Contrarily, to the results obtained by Monteiro *et al.* (2009) in which the young leaves are less sensitive to Cd toxicity because these leaves did not display variations on the chl *a*, *b* content and on the chlorophyll fluorescence parameters. Ahmed *et al.* (1983) study the effect of a systemic fungicide (benomyl) in sunflower plants. The contents of Chl *a*, Chl *b* and carotenoids in

treated sunflower leaves were considerably reduced. Moreover, these authors found that Chl *a* biosynthesis was more suppressed by benomyl treatment than the Chl *b*. In the same way our results show that the expanded leaves only had a significant reduction on the Chl *a* content.

The carotenoids act as light-harvesting pigments, and can protect chlorophyll and membrane destruction by quenching triplet chlorophyll and removing oxygen from the excited chlorophyll-oxygen complex (Coudhury and Behera, 2001). Thus, chlorophyll concentration decrease may be also a result of the reduction of the photoprotective action of carotenoids observed on young leaves exposed to mancozeb (carotenoids content decrease). In agreement with our results, Saladin *et al.* (2003a) observed that the plants exposed to the herbicide show leaf bleaching and necrosis areas at 21 days of exposure and a decrease in Chl and carotenoids concentration in *in vitro* grapevine plantlets exposed to the pesticide flumioxazin

Concerning the effects of mancozeb upon Chl *a* fluorescence parameters, which give information about the state of PSII, the young and expanded exposed leaves presented significant reduction on the photosynthetic efficiency (F_v/F_m) (Figure 3.27 A and B). Furthermore, the exposed expanded leaves showed a higher reduction of the quantum efficiency of PSII (Φ_{PSII}) than control leaves (Figure 3.27 C). By contrast, young leaves did not show any significant changes in the Φ_{PSII} (Figure 3.27 D).

The F_v/F_m values reflect the maximal efficiency of PSII and the decrease in this parameter indicates a reduction of the photosynthetic performance of mancozeb exposed lettuce leaves. However, despite these significant decreases, both, young and exposed leaves showed values within the range expected for healthy plants (Schreiber *et al.,* 1995). Analyses of the Φ_{PSII} revealed that only in the expanded leaves exposed to mancozeb the proportion of the light absorbed by chlorophyll associated with PSII that is used in photochemistry is reduced. This may be associated to the Chl *a* decreased observed in this leaves. Contrarily, in the young leaves, despite the deleterious effects of mancozeb in pigments contents, the effective photosynthetic efficiency of the lettuce plants exposed to mancozeb was not significantly affected. Thus, mancozeb exposure affected more markedly the photosynthetic performance of expanded leaves.

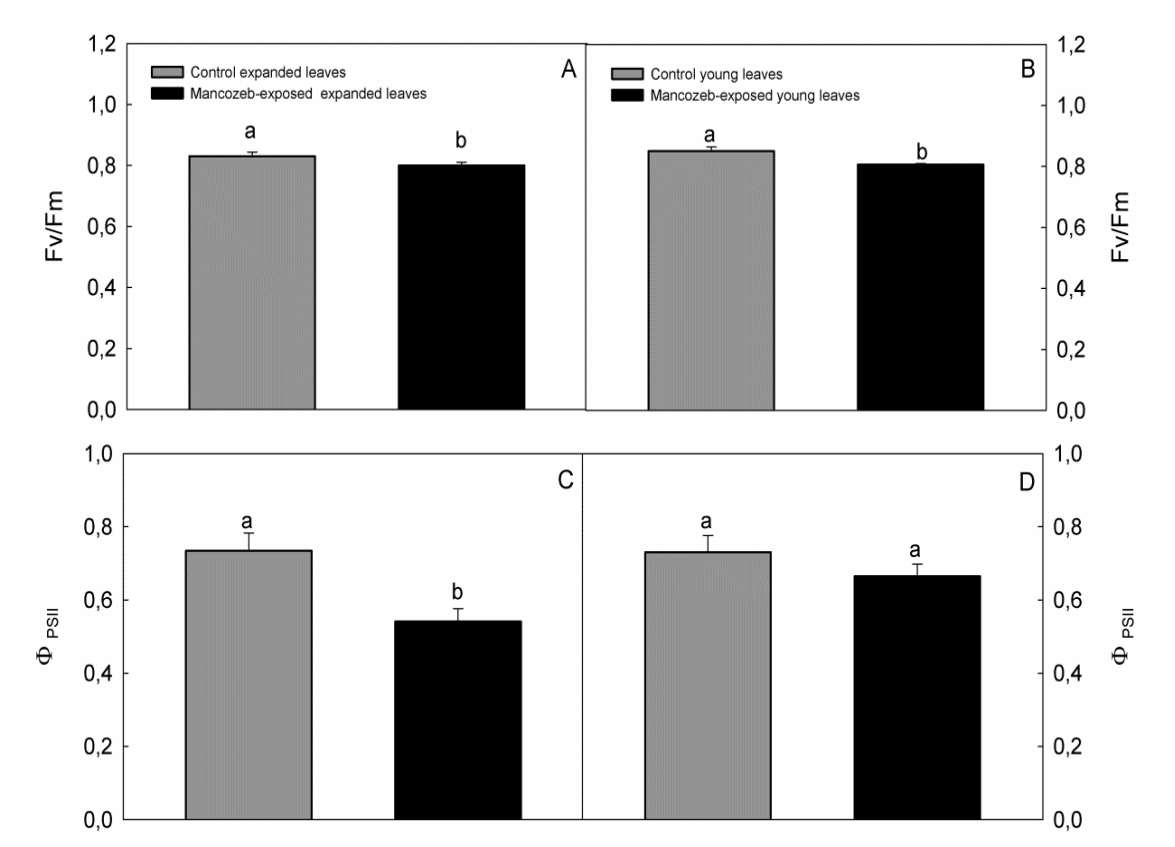

Figure 3.27: Effect of mancozeb stress on F_v/F_m and Φ_{PSII} in expanded and young leaves of lettuce. Values are means ± SD (n=6). Different letters indicate significant differences between treatments at a significant level equal to 0.05.

The Chl *a* fluorescence measurements appoint to an overall decrease of photosynthetic performance in lettuce leaves exposed to mancozeb. In mancozeb exposed expanded leaves, the photosynthetic apparatus were not able to cope with the reduction of Chl *a* decreasing its efficiency, while young leaves exposed to mancozeb were able to adapt and develop an efficient photosynthetic apparatus despite the reduced Chl *a*. Similar to the observed in the present work, the application of fludioxonil in grapevine plants induced a reduction of the Φ_{PSII} (Petit *et al.*, 2008). However, contrarily to the observed in lettuce, no significant changes were found in the F_v/F_m of grapevine. Lastly, Xia *et al.* (2006) reported that the exposure of cucumber plants to several systemic fungicides negatively affects Φ_{PSII} and F_v/F_m.

4. Conclusions and Future Work

In this work, the assignment of the ^{1}H HRMAS NMR spectra of lettuce leaves was performed through the use of 1D and 2D NMR experiments, and information found in literature which allowed the identification of 6 amino acids, 8 organic acids, glucose, fructose, sucrose, ethanol, methanol and choline.

In addition, it was observed the effect of EDTA in the lettuce NMR spectra. Our results indicate that addition of EDTA shows a trend in the improvement of the resolution of the signals on the spectra by effectively reducing the interaction of divalent metal ion such as calcium and magnesium with numerous metabolites. Nevertheless, the effect of EDTA depends on the composition of the sample, and the addition of peaks from free-EDTA and EDTA-metal complex obscured some peaks from endogenous metabolites.

It was also studied the changes that occur due to the aging of lettuce leaves. By ^{1}H HRMAS NMR spectroscopy the lettuce was found to be characterized by significant changes in many metabolites. The main differences are a higher content of sugars (glucose, sucrose and fructose) in young leaves and an increase of the malic and citric acid in expanded leaves. As expected, no significant changes in the pigments content and in the fluorescence measurements were found in young and expanded leaves.

Considering the results obtained in this work for the study of the effect of light/dark conditions during the growth of the plant, the absence of light (dark conditions) greatly contributes to compositional differences between expanded and young leaves. For instance, only in young leaves grown in dark conditions, is it recognizable two broad resonances at 1.37 and 2.21 ppm, with multiplicity of a triplet and singlet respectively. As a response to the dark growth conditions, the leaves presented lower contents of malic acid, higher contents of sugar (glucose and sucrose), an increase of unassigned systems from 7.00 to 7.44, and from 8.0 to 7.90 ppm which suggest the presence of phenolic compounds. In addition, the impact of the growth in dark conditions is more intense in the expanded leaves. In concordance with these results, the pigments concentration and the photosynthetic efficiency measurements, of leaves grown in dark conditions, were affected. Moreover, the photosynthetic performance of expanded leaves growing under dark conditions was more affected than young leaves under the same growth conditions.

Overall, the results show that treatment of lettuce leaves with mancozeb relatively to controls results in an increase of sugars (glucose and sucrose), in a decrease of amino acids (valine and alanine) and a decrease of lactic and fumaric acid. Throughout the

physiologic parameters studied, the results demonstrated that mancozeb exposure affected more markedly the photosynthetic performance of expanded leaves. Since the principal end products of photosynthesis are sugars and a decrease in this process was more noticeable in expanded leaves exposed to mancozeb, the increase of the sugars in these leaves was unexpected.

In the future, the confirmation of these results, through studies on the RuBisco enzyme activity (an important enzyme used in Calvin cycle), on the soluble carbohydrates content, and the use of multivariate analysis may allow a clear understanding of the variations that occur in the plant metabolism and physiology.

References

Ahmed, A.M., Heikal, M.D., Hinawy, O.S. (1983). Side effects of benomyl (fungicide) treatments on sunflower, cotton and cowpea plants. *Phyton (Austria)*, **23**: 185-195.

Alam, T.M., Alam, M.K., Neerathilingam, M., Volk, D.E., Sarkar, S., Ansari, G.A.S., Luxon, B.A. (2010). ^{1}H NMR metabonomic study of rat response to tri-phenyl phosphate and tri-butyl phosphate exposure. *Metabolomics,* **6**: 386-394.

Ali, K., Maltese, F., Zyprian, E., Rex, M., Choi, Y.H., Verpoorte, R. (2009). NMR metabolic fingerprinting based identification of grapevine metabolites associated with downy mildew resistance. *Journal of Agricultural and Food Chemistry,* **57**: 9599-9606.

Asiago, V.M., Gowda, G.A.N., Zhang, S., Shanaiah, N., Clark, J., Raftery, D. (2008). Use of EDTA to minimize ionic strength dependent frequency shifts in the ^{1}H NMR spectra of urine. *Metabolomics,* **4**: 328–336.

Aue, W.P., Bartholdi, E., Ernst R.R. (1976). Two-dimensional spectroscopy: Application to nuclear magnetic resonance. *Journal of Chemical Physics,* **64**: 2229-2246.

Barton, R.H., Waterman, D., Bonner, F.W., Holmes, E., Clarke, R., Procardis, C., Nicholson, J.K., Lindon, J.C. (2010). The influence of EDTA and citrate anticoagulant addition to human plasma on information recovery from NMR-based metabolic profiling studies. *Molecular Biosystems,* **6**: 215-224.

Baryla, A., Carrier, P., Franck, F., Coulomb, C., Sahut, C., Havaux, M. (2001). Leaf chlorosis in oilseed rape plants (*Brassica napus*) grown on cadmium-polluted soil: causes and consequences for photosynthesis and growth. *Planta,* **212**: 696-709.

Beger, R.D., Sun, J., Schnackenberg, L.K. (2010). Metabolomics approaches for discovering biomarkers of drug-induced hepatotoxicity and nephrotoxicity. *Toxicology and Applied Pharmacology*, **243**: 154–166.

Bertamini, M., Muthuchelian, K., Nedunchezhian, N. (2006). Shade effect alters leaf pigments and photosynthetic responses in Norway spruce (*Picea abies* L.) grown under field conditions. *Photosynthetica,* **44**: 227-234.

Blasco, C., Font, G, Picó, Y. (2004). Determination of dithiocarbamates and metabolites in plants by liquid chromatography–mass spectrometry. *Journal of Chromatography*, **1028**: 267-276.

Bodenhausen, G., Ruben, D.J. (1980). Natural abundance nitrogen-15 NMR by enhanced heteronuclear spectroscopy. *Chemical Physics Letters*, **69**: 185-188.

Braunschweiler, L., Bodenhausen, G., Ernst, R.R. (1983). Coherence transfer by isotropic mixing: application to proton correlation spectroscopy. *Journal of Magnetic Resonance*, **53**: 521-528.

Breitmaier, E. (2002). *Structure elucidation by NMR in organic chemistry*. 3nd edition, John Wiley & Sons Inc. United States of America.

Brewin, S., Miller, C., Khoshab, A. (2008). *7th European Pesticide Residues Workshop (EPRW).* Book of Abstracts, Germany.

Caldas, E.D., Miranda, M.C.C., Conceição, M.H., Souza, L.C.K.R. (2004). Dithiocarbamates residues in Brazilian food and the potential risk for consumers. *Food and Chemical Toxicology*, **42**: 1877-1883.

Choi, Y.H., Tapias, E.C., Kim, H.K., Lefeber, A.W.M., Erkelens, C., Verhoeven, J, Brzin, J., Zel, J., Verpoorte, R. (2004). Metabolic Discrimination of Catharanthus roseus Leaves Infected by Phytoplasma Using ^{1}H-NMR Spectroscopy and Multivariate Data Analysis. *Plant Physiology*, **135**: 2398–2410.

Choudhury, N.K., Behera, R.K. (2001). Photoinhibition of photosynthesis: role of carotenoids in photoprotection of chloroplast constituents**.** *Photosynthetica*, **39:** 481-488.

Claridge, T.D.W. (2009). *High-Resolution NMR techniques in organic chemistry*. 2nd edition, Elsevier Academic press. United States of America. ISBN-13: 978-0-08-054628-5.

Colquhoun, I.J. (2007). Use of NMR for metabolic profiling in plant systems. *Journal of Pesticide Science*, **32**: 200–212.

Crnogorac, G., Schwack, W. (2007). Determination of dithiocarbamate fungicide residues by liquid chromatography/mass spectrometry and stable isotope dilution assay. *Rapid Communications in Mass Spectrometry*, **21**: 4009-4016.

Crnogorac, G., Schwack, W. (2009). Residue analysis of dithiocarbamate fungicides. *Trends in Analytical Chemistry,* **28**: 40-50.

Dias, M.C., Monteiro, C., Moutinho-Pereira, J., Correia, C., Gonçalves, B., Santos, C. (2011). Photosynthetic targets of cadmium toxicity: a case study with the plant model *Lactuca sativa*. *Submitted to "*Ecotoxicology *and Environmental Safety".*

Duarte, I.F., Delgadillo, I., Gil, A.M. (2006). Study of natural mango juice spoilage and microbial contamination with *Penicillium expansum* by high resolution ^{1}H NMR spectroscopy. *Food Chemistry*, **96**: 313-324.

Duarte, I.F., Lamego, I., Marques, J., Marques, P.M., Blaise, B.J., Gil, A.M. (2010). Nuclear Magnetic Resonance (NMR) study of the effect of cisplatin on the metabolic profile of MG-63 osteosarcoma cells. *Journal of Proteome Research,* **9**: 5877–5886.

DuPont, M.S., Mondin, Z., Williamson, G., Price, K.R. (2000). Effect of variety, processing, and storage on the flavonoid glycoside content and composition of lettuce and endive. *Journal of Agricultural and Food Chemistry,* **48**: 3957-3964.

EFSA. (2009). *Annual Report on Pesticide Residues.* EFSA- European Food Safety Authority. 1-106.

EHU. (2002). *Carbamate Pesticides*. EHU- Environmental Health Unit. Queensland. 1-4.

Ferreira, A. (2007). *Exposição de Crómio em alface: acumulação e efeitos na fisiologia e genotoxicidade.* Tese de Mestrado em Toxicologia e Ecotoxicologia. Universidade de Aveiro, Aveiro. 1-79.

Fukumoto, L.R., Toivonen, P.M., Delaquis, P.J. (2002). Effect of wash water temperature and chlorination on phenolic metabolism and browning of stored iceberg lettuce photosynthetic and vascular tissues. *Journal of Agricultural and Food Chemistry*, **50**: 4503-4511.

Gaw, S.K., Kim, N.D., Northcott, G.L., Wilkins, A.L., Robinson, G. (2008). Uptake of ΣDDT, arsenic, cadmium, copper, and lead by lettuce and radish grown in contaminated horticultural soils. *Journal of Agricultural and Food Chemistry,* **56**: 6584-6593.

Graça, G., Duarte, I.F., Barros, A.S., Goodfellow, B.J., Diaz, S., Carreira, I.M., Couceiro, A.B., Galhano, E., Gil, A.M. (2009). ^{1}H NMR based metabonomics of human amniotic fluid for the metabolic characterization of fetus malformations. *Journal of Proteome Research,* **8**: 4144-4150.

Griffin, J.L. (2004). The potential of metabonomics in drug safety and toxicology. Em: L. Kelvin and H. Timmerman (eds). *Drug Discovery Today: Technologies*, **1**: 285-293.

Griffiths, G., Leverentz, M., Silkowski, H., Gill, N., Sanchez-Serrano, J.J. (2000). Lipid hydroperoxide levels in plant tissues. *Journal of Experimental Botany*, **51**: 1363-1370.

Griffiths, W.J., Wang, Y. (2008). Mass spectrometry: from proteomics to metabolomics and lipidomics. *Chemical Society Reviews*, **38**: 1882-1896.

Gupta, C.R. (2006). *Toxicology of organophosphate and carbamate compounds.* Elsevier Academic press. United States of America. ISBN: 0-12-088523-9.

Han, S., Ba, Y. (2004). Determination of the concentrations of metal cations in aqueous solutions using proton nmr spectral area integration of the edta complexes. *Journal of Solution Chemistry,* **33**: 301-312.

Han, S., Mathias, E.V., Ba, Y. (2007). Proton NMR determination of Mg^{2+} and Ca^{2+} concentrations using tetrasodium EDTA complexes. *Journal of Chemistry,* **1:** 1-5.

Houeto, P., Bindoula, G., Hoffman, J.R. (1995). Ethylenebisdithiocarbamates and ethylenethiourea: Possible human health hazards. *Environmental Health Perspectives*, **103**: 568-573.

Huang, B., Kuo, S., Bembenek, R. (2005). Availability to lettuce of arsenic and lead from trace element fertilizers in soil. *Water, Air, and Soil Pollution,* **164**: 223–239.

ISO. (1993). *Soil quality-determination of the effects of pollutants on soil flora-part 1: methods for the measurement of inhibition of root growth*. ISO- International organization for standardization. Genéve. 1-9.

ISO. (1995). *Soil quality-determination of the effects of pollutants on soil flora-part 2: effects of chemicals on the emergence of higher plants*. ISO- International organization for standardization. Genéve. 2-7.

Jacobsen, N.E. (2007). *NMR spectroscopy explained: Simplified theory, applications and examples for organic chemistry and structural biology.* John Wiley & Sons Inc. United States of America. ISBN: 978-0-471-73096-5.

Kimura, M., Rodriguez-Amaya, D.B. (2003). Carotenoid composition of hydroponic leafy vegetables. *Journal of Agricultural and Food Chemistry,* **51**: 2603-2607.

Krieger, R. (2010). *Hayes' handbook of pesticide toxicology*. Em: J. Doull, J. van Hemmen, E. Hodgson, H. Maibach, L. Reiter, L. Ritter, J. Ross, W. Slikker (eds.). 3nd edition, Elsevier Academic press. United States of America. ISBN: 978-0-12-374481-4.

Krishnan, P., Kruger, N.J., Ratcliffe, R.G. (2005). Metabolite fingerprinting and profiling in plants using NMR. *Journal of Experimental Botanic*, **56**: 255-265.

Kumar, R., Kaushal, S., Shukla, Y.R. (2010). Variability, correlation, and path analysis studies in lettuce. *International Journal of Vegetable Science*, **16**: 299-315.

Lichtenthaler, H.K., Alexander, A.C., Marek, A., Kalina, M.V., Urban, O. (2007). Differences in pigment composition, photosynthetic rates and chlorophyll fluorescence images of sun and shade leaves of four tree species. *Plant Physiology and Biochemistry*, **45**: 577-588.

Lima, M.R.M., Felgueiras, M.L., Graça, G., Rodrigues, J.E.A., Barros, A., Gil, A.M., Dias, A.C.P. (2010). NMR metabolomics of esca disease-affected *Vitis vinifera* cv. Alvarinho leaves. *Journal of Experimental Biology,* **61**: 1-10.

Lin, X., Chen, X., Huo, X., Yu, Z., Bi, K., Li, Q. (2011). Dispersive liquid–liquid microextraction coupled with high-performance liquid chromatography-diode array detection for the determination of *N*-methyl carbamate pesticides in vegetables. *Journal of Separation Science,* **34**: 202-209.

Lindon, J.C., Beckonert, O.P., Holmes, E., Nicholson, J.K. (2009). High-resolution magic angle spinning NMR spectroscopy: Application to biomedical studies. *Progress in Nuclear Magnetic Resonance Spectroscopy,* **55**: 79-100.

Lindon, J.C., Nicholson, J.K. (2008). Analytical technologies for metabonomics and metabolomics, and multi-omic information recovery. *Trends in Analytical chemistry*, **27**: 194-204.

Lindon, J.C., Nicholson, J.K. (2008a). Spectroscopic and statistical techniques for information recovery in metabonomics and metabolomics. *Annual Review of Analytical chemistry,* **1**: 45-69.

Lindon, J.C., Nicholson, J.K., Holmes, E. (2007). *The handbook of metabonomics and metabolomics.* Elsevier Academic press. The Netherlands. ISBN: 0-444-52841-5.

Liu, M, Nicholson, J.K., Lindon, J.C. (1996). High-resolution diffusion and relaxation edited one- and two-dimensional ^{1}H NMR spectroscopy of biological fluids. *Analytical Chemistry,* **68**: 3370-3376.

Martin, C.E., Hsu, R.C., Lin, T.C. (2010). Sun/shade adaptations of the photosynthetic apparatus of *Hoya carnosa*, an epiphytic CAM vine, in a subtropical rain forest in northeastern Taiwan. *Acta Physiologiae Plantarum,* **32**: 575–581.

Merhi, M., Demur, C., Racaud-Sultan, C., Bertrand, J., Canlet, C., Blas, F., Estrada, Y., Gamet-Payrastre, L. (2010). Gender-linked haematopoietic and metabolic disturbances induced by a pesticide mixture administered at low dose to mice. *Toxicology,* **267**: 80-90.

Monteiro, M.S., Rodriguez, E., Loureiro, J., Mann, R.M., Soares, A.M.V.M., Santos, C. (2010). Flow cytometric assessment of Cd genotoxicity in three plants with different metal accumulation and detoxification capacities. *Ecotoxicology and Environmental Safety,* **73**: 1231-1237.

Monteiro, M.S., Santos, C., Soares, A.M.V.M., Mann, R.M. (2009). Assessment of biomarkers of cadmium stress in lettuce. *Ecotoxicology and Environmental Safety,* **72**: 811-818.

Mukerji, K.G. (2004). Fruit and vegetable diseases. Kluwer Academic Publishers. United States of America. ISBN: 1-4020-1976-9.

Mulkey, M.E. (2001). *Thiocarbamates: A determination on the existence of a common mechanism of toxicity and a screening level cumulative food risk assessment*. Office of Pesticide Programs. United States of America.

Nicholson, J.K., Conelly, J., Lindon, J.C., Holmes, E. (1999). 'Metabonomics': Understanding the metabolic responses of living systems to pathophysiological stimuli via multivariate statistical analysis of biological NMR spectroscopic data. *Xenobiotica,* **29**: 1181–1189.

Nicholson, J.K., Conelly, J., Lindon, J.C., Holmes, E. (2002). Metabonomics: a platform for studying drug toxicity and gene function. *Nature Reviews Drug Discovery,* **1**: 153-161.

Nicolle, C., Cardinault, N., Gueux, E., Jaffrelo, L., Rock, E., Mazur, A. (2004). Health effect of vegetable-based diet: lettuce consumption improves cholesterol metabolism and antioxidant status in the rat. *Clinical Nutrition,* **23**: 605–614.

Nielsen, J., Jewett, M.C. (2007). *Metabolomics: A powerful tool in systems biology.* Springer. Denmark. ISBN: 978-3-540-74718-5.

Oh, M.M., Carey, E.E., Rajashekar, C.B. (2009). Environmental stresses induce health-promoting phytochemicals in lettuce. *Plant Physiology and Biochemistry,* **47**: 578–583.

Oh., M., Trick, H.N., Rajashekar, C.B. (2009). Secondary metabolism and antioxidants involved in environmental adaptation and stress tolerance in lettuce. *Journal of Plant Physiology*, **166**: 180-191.

Oliver, S.G., Winson, M.K., Kell, D.B., Baganz, F. (1998). Systematic functional analysis of the yeast genome. *Trends in Biotechnology*, **16**: 373–378.

Pérez, E.M.S., Iglesias, M.J., Ortiz, F.L., Pérez I.S., Galera, M.M. (2010). Study of the suitability of HRMAS NMR for metabolic profiling of tomatoes: Application to tissue differentiation and fruit ripening. *Food Chemistry*, **122**: 877-887.

Petit, A-N., Fontaine, F., Clément, C., Vaillant-Gaveau, N. (2008). Photosynthesis limitations of grapevine after treatment with the fungicide fludioxonil. *Journal of Agricultural and Food Chemistry,* **56**: 6761-6767.

Pystina, N.V., Danilov, R.A. (2001). Influence of light regimes on respiration, activity of alternative respiratory pathway and carbohydrates content in mature leaves of ajuga reptans. *Revista Brasileira de Fisiologia Vegetal,* **13**: 285-292.

Razinger, J., Drinovec, L., Zrimec, A. (2010). Real-time visualization of oxidative stress in a floating macrophyte *Lemna minor* L. exposed to cadmium, copper, menadione, and AAPH. *Environmental Toxicology*, **25**: 573-580.

Ritota, M., Marini, F., Sequi, P., Valentini, M. (2010). Metabolomic characterization of Italian sweet pepper (*Capsicum annum* L.) by means of HRMAS-NMR spectroscopy and multivariate analysis. *Journal of Agricultural and Food Chemistry,* **58**: 9675–9684.

Romani, A., Pinelli, P., Galardi, C., Sani, G., Cimato, A., Heimler, D. (2002). Polyphenols in greenhouse and open-air-grown lettuce. *Food Chemistry,* **79**: 337–342.

Rosa, M., Prado, C., Podazza, G., Interdonato, R., González, J.A., Hilal, M., Prado, F.E (2009). Soluble sugars-metabolism, sensing and abiotic stress: A complex network in the life of plants. *Plant Signaling & Behaviour,* **4**: 388–393.

Saladin, G., Clément, C., Magné, C. (2003a). Stress responses of grapevine to flumioxazin herbicide involves dehydration, cell membrane, alteration and osmoregulation process. *Plant Cell Reports*, **21**: 1221-1227.

Saladin, G., Magné, C., Clément, C. (2003). Impact of flumioxazin herbicide on growth and carbohydrate physiology in *Vitis vinifera* L. *Plant Cell Reports*, **21**: 821–82.

Schreiber, U., Endo, T., Mi, H., Asada, K. (1995). Quenching analysis of chlorophyll fluorescence by the saturation pulse method: particular aspects relating to the study of eukaryotic algae and cyanobacteria. *Plant and Cell Physiology,* **36**: 873-882.

Schwender, J. (2009). *Plant metabolic networks.* Em: U. Roessner and D.M. Beckles (eds.). Springer. United States of America. ISBN 978-0-387-78744-2.

Serafini, M., Bugianesi, R., Salucci, M., Azzini, E., Raguzzini A., Maiani, G. (2002). Effect of acute ingestion of fresh and stored lettuce (*Lactuca sativa*) on plasma total antioxidant capacity and antioxidant levels in human subjects. *British Journal of Nutrition*, **88**: 615–623.

Shuib, N.H., Shaaru, K., Khatib, A., Maulidiani, A., Kneer, R., Zareen, S., Mohd, S., Raof, A., Nordin, H., Lajis, Neto, V. (2011). Discrimination of young and mature leaves of *Melicope ptelefolia* using ^{1}H NMR and multivariate data analysis. *Food Chemistry*, **126**: 640–645

Sims, D.A., Gamon, J.A. (2002). Relationships between leaf pigment content and spectral reflectance across a wide range of species, leaf structures and developmental stages. *Remote Sensing of Environmental*, **81**: 337–354.

Sobolev, A.P., Brosio, E., Gianferri, R., Segre, A.L. (2005). Metabolic profile of lettuce leaves by high-field NMR spectra. *Magnetic Resonance in Chemistry*, **43**: 625-638.

Sobolev, A.P., Segre, A., Lamanna, R. (2003). Proton high-field NMR study of tomato juice. *Magnetic Resonance in Chemistry*, **41**: 237-245.

Sobolev, A.P., Testone, G., Santoro, F., Nicolodi, C., Ianneli, M.A., Amato, M.E., Iannello, A., Brosio, E., Giannino, D., Mannina, L. (2010). Quality traits of conventional and transgenic lettuce (*Lactuca sativa* L.) at harvesting by NMR metabolic profiling. *Journal of Agricultural and Food Chemistry*, **58**: 6928-6936.

Sumner, L.W., Mendes, P., Dixon, R.A. (2003). Plant metabolomics: large-scale phytochemistry in the functional genomics era. *Phytochemistry*, **62**: 817–836.

Tavares, H.M.R. (1988). *A cultura da alface*. Ministério da Agricultura, Pescas e Alimentação. Lisboa.

Teng, Q. (2005). *Structural biology: practical NMR applications*. Springer Science and Business Media Inc. United States of America. ISBN: 0-387-24367-4.

Trautmann, N.M., Carlsen, W.S., Krasny, M.E., Cunningham, C.M. (2001). *Assessing toxic risk.* Student edition, National Science Teachers Association press. United States of America. ISBN: 0-87355-196-6.

Untiedt, R., Blanke, M.M. (2004). Effects of fungicide and insecticide mixtures on apple tree canopy photosynthesis, dark respiration and carbon economy. *Crop Protection* , **23**: 1001-1008.

van Kooten, O., Snel, J.F.H., (1990). The use of chlorophyll fluorescence nomenclature in plant stress physiology. *Photosynthesis Research*, **25**: 47–150.

van Lishaut, H., Schwack, W. (2000). Selective trace determination of dithiocarbamate fungicides in fruits and vegetables by reversed-phase ion-pair liquid chromatography with ultraviolet and electrochemical detection. *The Journal of AOAC International*, **83**: 720-727.

Villas-Bôas, S.G., Mas, S., Akesson, M., Smedsgaard, J., Nielsen J. (2005). Mass spectrometry in metabolome analysis. *Journal of Mass Spectrometry*, **24**: 613-646.

Wang, Y., Gao, L., Wang, Z., Liu, Y., Sun, M., Yang, D., Wei, C., Shan, Y., Xia, T. (2011). Light-induced expression of genes involved in phenylpropanoid biosynthetic pathways in callus of tea (*Camellia sinensis* (L.) O. Kuntze). *Scientia Horticulturae*, **133**: 72-83.

Ward, J.L., Baker, J.M., Beale, M.H. (2007). Recent applications of NMR spectroscopy in plant metabolomics. *The FEBS Journal*, **274**: 1126–1131.

Weybright, P., Millis, K., Campbell, N., Cory, D.G., Singer, S. (1998). Gradient, high-resolution, magic angle spinning ^{1}H nuclear magnetic resonance spectroscopy of intact cells. *Magnetic Resonance in Medicine*, **39**: 337-345.

Whitehead, D., Barbour, M.M., Griffin, K.L., Turnbull, M.H., Tissues, D.T. (2011). Effects of leaf age and tree size on stomatal and mesophyll limitations to photosynthesis in mountain beech (*Nothofagus solandrii* var. *cliffortiodes*). *Tree Physiology*, **31:** 985-996.

Winter, M., Hermann, K. (1986). Esters and glucosides of hydroxycinnamic acids in vegetables. *Journal of Agricultural and Food Chemistry*, **34**: 616-620.

Xia, X., Huang, Y., Wang, L., Huang, L, Yun Long, Y., Yu, J. (2006). Pesticides-induced depression of photosynthesis was alleviated by 24-epibrassinolide pretreatment in *Cucumis sativus* L. *Pesticide Biochemistry and Physiology*, **86**: 42-48.

Zorrig, W., Rouached, A., Shahzad, Z., Abdelly, C., Davidian, J.C., Berthomieu, P. (2010). Identificaton of three relationships linking cadmium accumulation to cadmium tolerance and zinc and citrate accumulation in lettuce. *Journal of Plant Physiology*, **167**: 1239-1247.